N63 21728

33

MTP-AERO-63-29
April 24, 1963

GEORGE C. MARSHALL SPACE FLIGHT CENTER

HUNTSVILLE, ALABAMA

A SURVEY OF THE INFLUENCE OF VARIATIONS IN STAGE CHARACTERISTICS ON OPTIMIZED TRAJECTORY SHAPING

PART I: TWO STAGE VEHICLE INJECTION INTO CIRCULAR ORBITS

M. C. Davidson Jr.

OTS PRICE

XEROX $

MICROFILM $

FOR INTERNAL USE ONLY

NATIONAL AERONAUTICS AND SPACE ADMINISTRATION

GEORGE C. MARSHALL SPACE FLIGHT CENTER

MTP-AERO-63-29

A SURVEY OF THE INFLUENCE OF VARIATIONS IN STAGE CHARACTERISTICS ON OPTIMIZED TRAJECTORY SHAPING

PART I: TWO STAGE VEHICLE INJECTION INTO CIRCULAR ORBITS

By M. C. Davidson, Jr.

ABSTRACT

The purpose of this study is to infer the effects of second stage engine characteristics on trajectory shape, weight at cutoff, and optimum control histories of the second stage for a two stage vehicle fulfilling circular orbit mission criteria. The first stage was taken to be an S-I booster and the second stage is defined by an initial thrust to weight ratio, F/w_o, and a specific impulse, I_{sp}, value. Circular orbit missions were considered at 100, 200, and 300 km altitudes.

By the consideration of the value of a parameter at the terminal point of the trajectory, we can systematically study the geometrical shape of the trajectory.

Weight at cutoff is shown as a function of F/w_o for different I_{sp} values, circular injection altitudes, and first stage tilt programs.

Examples of optimum control histories for the second stage are given.

GEORGE C. MARSHALL SPACE FLIGHT CENTER

MTP-AERO-63-29

April 24, 1963

A SURVEY OF THE INFLUENCE OF VARIATIONS IN STAGE CHARACTERISTICS ON OPTIMIZED TRAJECTORY SHAPING

PART I: TWO STAGE VEHICLE INJECTION INTO CIRCULAR ORBITS

By

M. C. Davidson, Jr.

FUTURE PROJECTS BRANCH
AEROBALLISTICS DIVISION

TABLE OF CONTENTS

GEORGE C. MARSHALL SPACE FLIGHT CENTER

MTP-AERO-63-29

A SURVEY OF THE INFLUENCE OF VARIATIONS IN STAGE CHARACTERISTICS ON OPTIMIZED TRAJECTORY SHAPING

PART I: TWO STAGE VEHICLE INJECTION INTO CIRCULAR ORBITS

By M. C. Davidson, Jr.

SUMMARY

The purpose of this study is to infer the effects of second stage engine characteristics on trajectory shape, weight at cutoff, and optimum control histories of the second stage for a two stage vehicle fulfilling circular orbit mission criteria. The first stage was taken to be an S-I booster and the second stage is defined by an initial thrust to weight ratio, F/w_o, and a specific impulse, I_{sp}, value. Circular orbit missions were considered at 100, 200, and 300 km altitudes.

By the consideration of the value of a parameter at the terminal point of the trajectory, we can systematically study the geometrical shape of the trajectory.

Weight at cutoff is shown as a function of F/w_o for different I_{sp} values, circular injection altitudes, and first stage tilt programs.

Examples of optimum control histories for the second stage are given.

SECTION I. PROBLEM DESCRIPTION AND OUTLINE OF APPROACH

We are to study the effects of second stage engine characteristics on trajectory shape, weight into orbit, and optimum control histories of a two stage vehicle fulfilling circular orbit mission criteria. In particular, the first stage is taken to be an S-I booster flying in two dimensions a one parameter set of angle of attack programs in the environment of a spherical non-rotating earth with atmosphere. The second stage initial conditions are obtained by adding the earth's rotational effect at cutoff of the first stage under the assumption of a ninety degree azimuth at launch. The second stage is to fly a two dimensional calculus of variation path, minimizing the time of flight, in the gravitational field of a spherical earth free of atmosphere. In a (r, v, ϑ) coordinate system, the particular three first stages we are to study give initial conditions for the second stage of

$$\left.\begin{array}{lll} y_o = 76.87 \text{ (km)} & y_o = 70.37 \text{ (km)} & y_o = 63.21 \text{ (km)} \\ v_o = 2884 \text{ (m/s)} & v_o = 2937 \text{ (m/s)} & v_o = 2991 \text{ (m/s)} \\ \vartheta_o = 63.8 \text{ (deg)} & \vartheta_o = 68.1 \text{ (deg)} & \vartheta_o = 72.4 \text{ (deg)} \end{array}\right\} \quad (1)$$

where y is the altitude, $y = r - R_o$, R_o being the radius of the earth. We will refer to these first stage end conditions by their earth-fixed theta values, $\vartheta_I = 60$, 65, and 70 degrees, respectively.

We wish to connect these initial conditions, (1), through a continuous burning second stage characterized by an initial thrust to weight ratio, F/w_o, and a specific impulse, I_{sp}, value to circular orbit conditions at altitudes of $y_c = 100$, 200, and 300 km. The variation in lift-off weight produced by varying the weight of the second stage in the form F/w_o is ignored. The selection of a ϑ_I, F/w_o, I_{sp}, and y_c leads to a discrete minimal time calculus of variation second stage trajectory. The method of constructing such a trajectory is a numerical isolation procedure determining the initial values of the angle of attack and its time derivative, α_o and $\dot{\alpha}_o$. This is a numerical procedure for solving the two point boundary value problem. The four parameters of the study are taken to have the following restriction on their values:

$$\left.\begin{aligned} &\vartheta_I = 60,\ 65,\ \text{and}\ 70\ \text{(deg)} \\ &.5 \leqq F/w_o \leqq 2.0 \\ &I_{sp} \leqq 1500\ \text{(sec)} \\ &y_c = 100,\ 200,\ \text{and}\ 300\ \text{(km)} \end{aligned}\right\} \tag{2}$$

The following section deals with the physical shape of the trajectory.

SECTION II. TRAJECTORY SHAPE

This section deals with the geometrical shape of the trajectory. In order to explain the classification, let us consider the equations of motion for the second stage. In a $(r,\ v,\ \vartheta)$ coordinate system, they are as follows:

$$\begin{aligned} \dot{r} &= v \cos \vartheta \\ \dot{v} &= F/m \cos \alpha - g \cos \vartheta \\ \dot{\vartheta} &= \frac{1}{v}\left\{F/m \sin \alpha + \left(g - \frac{v^2}{r}\right) \sin \vartheta\right\} \end{aligned} \tag{3}$$

where F is the thrust magnitude, m is the instantaneous mass, and g is the magnitude of the local gravity force. Differentiating the first of (3) gives

$$\ddot{r} = \dot{v} \cos \vartheta - v\, \dot{\vartheta} \sin \vartheta\ . \tag{4}$$

Now let us examine the second stage trajectory as it enters the injection or cutoff point. The conditions for circular injection are

$$\vartheta_c = 90\ \text{deg} \quad \text{and} \quad g = \frac{{v_c}^2}{r_c} \tag{5}$$

where r_c is the radius of injection. Now let us evaluate (3) and (4) at this point common to trajectory and orbit. We obtain from (3)

$$\dot{r}_c = 0 \ , \quad \dot{v} = \frac{F}{m} \cos \alpha_c \ , \quad \text{and } \dot{\vartheta}_c = \frac{F}{m\, v_c} \sin \alpha_c \ , \qquad (6)$$

and (4) becomes

$$\ddot{r}_c = - v_c \, \dot{\vartheta}_c \ . \qquad (7)$$

Combining (6) and (7) we have

$$\ddot{r}_c = - \frac{F}{m} \sin \alpha_c \ . \qquad (8)$$

Now assume we have applied the calculus of variations to minimize the time of flight subject to the differential equation constraints, (3), and with the particular values of y_c, ϑ_I, F/w_o, and I_{sp} choosen, the solution to the two point boundary value problem yields a trajectory with an angle of attack at cutoff, α_c, of zero. Equation (8) states $\ddot{r}_c = 0$, or that the trajectory is flat in the neighborhood of cutoff; here we assume that the range on the trajectory is a monotonic increasing function of time. If we assume conditions which lead to an $\alpha_c > 0$, hence $\ddot{r}_c < 0$, the trajectory is concave down at cutoff. In this case the vehicle entered the circular orbit from below. In a similar manner if $\alpha_c < 0$ we have a concave up trajectory entering the orbit from above.

Next, let us introduce a notation to express the general character of the trajectory shape: we say a trajectory is of class T_n if it has crossed the desired free flight orbit, in this case a circle, exactly n times prior to cutoff. Since in our study all initial altitudes of the second stage are less than the lowest circular altitude considered (100 km), the T_o, T_2, T_4... trajectories inject from below and have $\alpha_c > 0$. Similarly the T_1, T_3, T_5... trajectories inject from above having $\alpha_c < 0$. Let us further denote a class dividing trajectory ($\alpha_c = 0$) by T_{ij}, where this trajectory divides

trajectories of class T_i and of class T_j $(i<j)$. For example, class T_0 has $\alpha_c > 0$, and class T_1 has $\alpha_c < 0$, then the dividing trajectory would be designated by T_{01} and have $\alpha_c = 0$. Here, of course, we are assuming the necessary functional properties between points on the trajectory and α_c.

For discussion let us fix the values of y_c, ϑ_I, and F/w_0 and examine the family of trajectories produced by allowing I_{sp} to take on different values. The study then proceeds by considering α_c as a function of I_{sp}, noting the values of I_{sp} for which $\alpha_c = 0$. These are the dividing trajectories. Here we should say that

$$\frac{d\,\alpha_c}{d\,I_{sp}} \neq 0 \ .$$

Figure 1 gives, as an example, this information for $y_c = 200$ km, $\vartheta_I = 65$ deg, and $F/w_0 = .5$. It is noted that two such dividing trajectories are encountered in the range of I_{sp} investigated, a T_{01} at $I_{sp} = 160$ and a T_{12} at $I_{sp} = 625$. Thus, we have the following classes of trajectories:

$$T_0 \ , \quad I_{sp} < 160$$

$$T_1 \ , \quad 160 < I_{sp} < 625$$

$$T_2 \ , \quad 625 < I_{sp} <$$

where the upper limit for T_2 type trajectories is not encountered. Figure 2 gives altitude as a function of range for this case. The broken lines indicate dividing trajectories, and the solid lines indicate typical examples for the classes encountered. Figures 3 through 11 give α_c as a function of I_{sp} for values of the parameters consistent with (2). These figures are to be compared with Figures 12 through 26 which illustrate the trajectory shapes.

The case of $F/w_0 = .5$ yields extreme convergency problems in the isolation scheme for higher values of I_{sp}: thus, some of the information for such cases is missing. For all values of F/w_0, I_{sp} was taken as low as practically possible.

In the next section, we give the weight at cutoff information.

SECTION III. WEIGHT AT CUTOFF

In this section we are to investigate cutoff weight for values of the parameters consistent with (2). Let us consider the normalized cutoff weight, w_c/w_o, where w_c is the actual cutoff weight and w_o is the initial weight of the second stage, as a function of F/w_o. This information is presented in Figures 27 through 47. Each figure corresponds to a different combination of the altitude of injection, y_c, and the I_{sp} value, while the curves of each figure are characterized by a first stage, ϑ_I.

We observe in many cases that there occurs a maximum of w_c/w_o with respect to F/w_o for fixed y_c, I_{sp}, and ϑ_I values. The optimization of w_c/w_o with respect to ϑ_I is not presented due to the small range of ϑ_I considered.

Although not included in this report, w_c/w_o as a function of I_{sp} reveals a monotonic increasing behavior.

The following section gives examples of the control histories.

SECTION IV. CONTROL HISTORIES

Here, we give typical examples of the angle of attack (α) and chi (χ) as a function of time on the trajectory. Chi is the angle measured from the vertical at launch to the vehicle longitudinal axis and is related to α as

$$\chi = \phi + \vartheta + \alpha \ ,$$

where ϕ is the central angle. Figures 48, 49, and 50 give examples of α as a function of time and Figures 51, 52, and 53 give the corresponding χ functions. It is noted that for high F/w_o and high I_{sp} values χ is nearly linear while this is not true for either low F/w_o or low I_{sp} values.

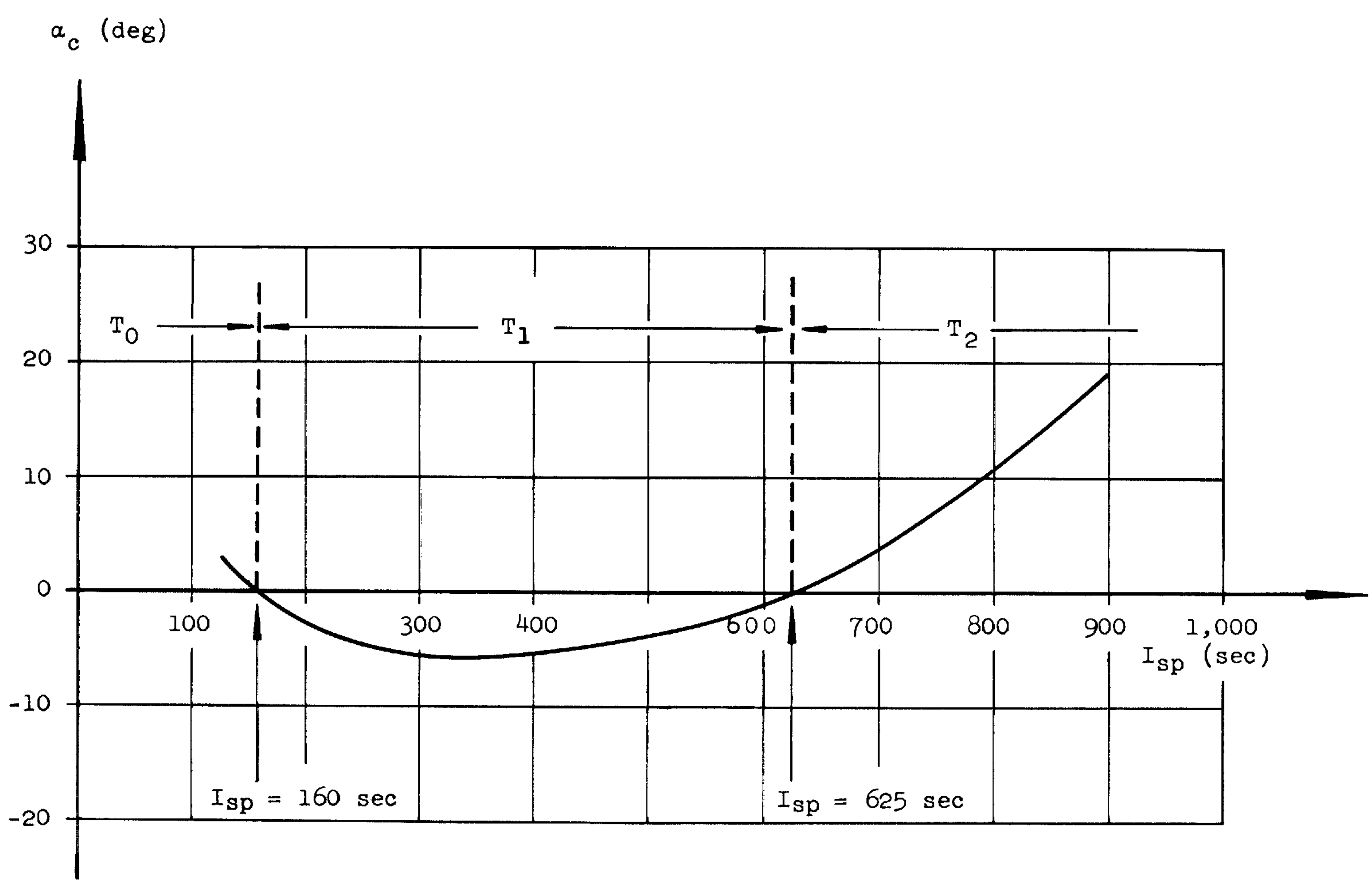

y_c = 200 km; ϑ_I = 65 deg; F/W_o = .5

ANGLE OF ATTACK AT CUTOFF (α_c) AS FUNCTION OF SPECIFIC IMPULSE
FIGURE 1

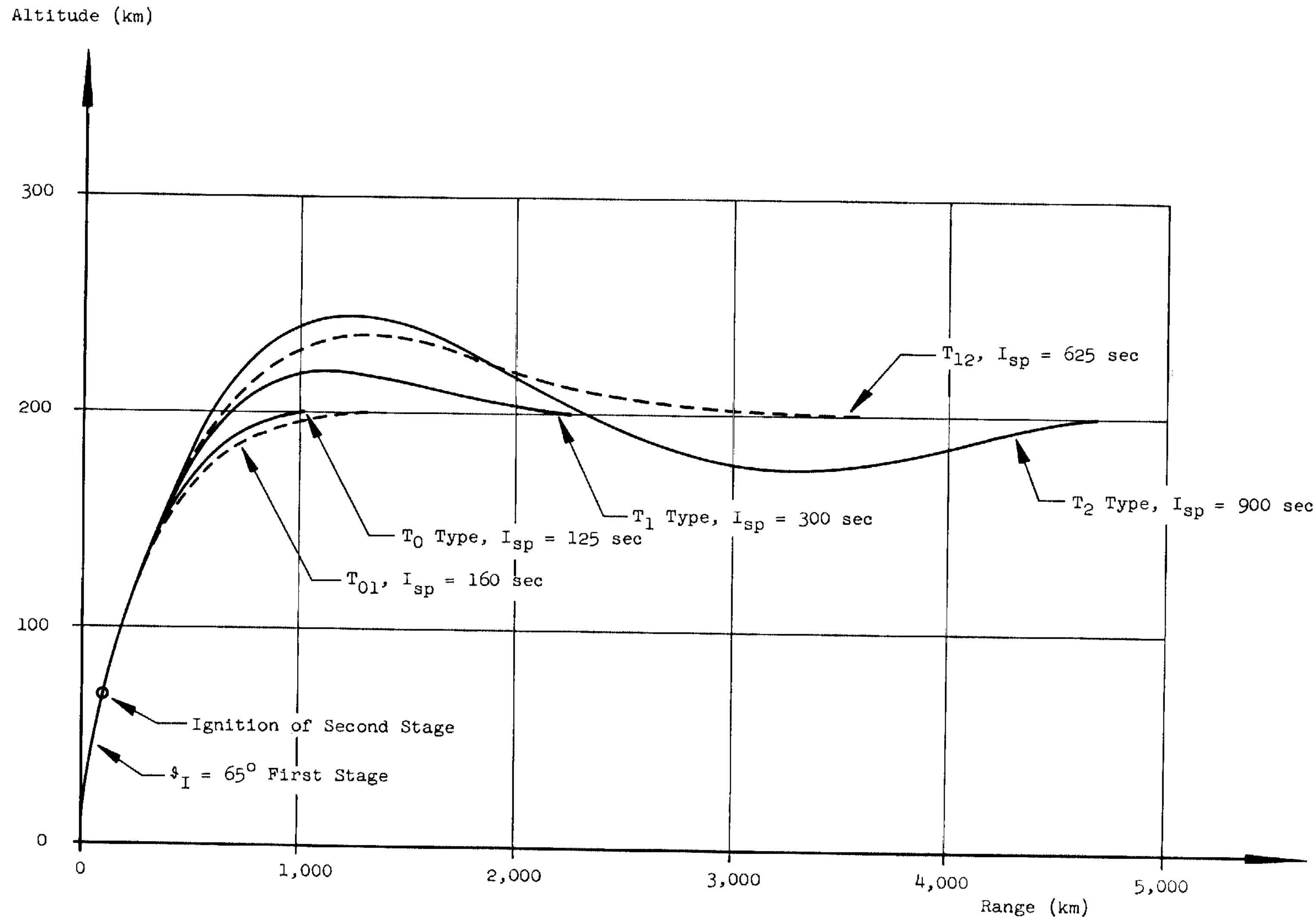

y_c = 200 km; ϑ_I = 65 deg; F/W_o = .5
GEOMETRY FOR THREE TRAJECTORY TYPES
FIGURE 2

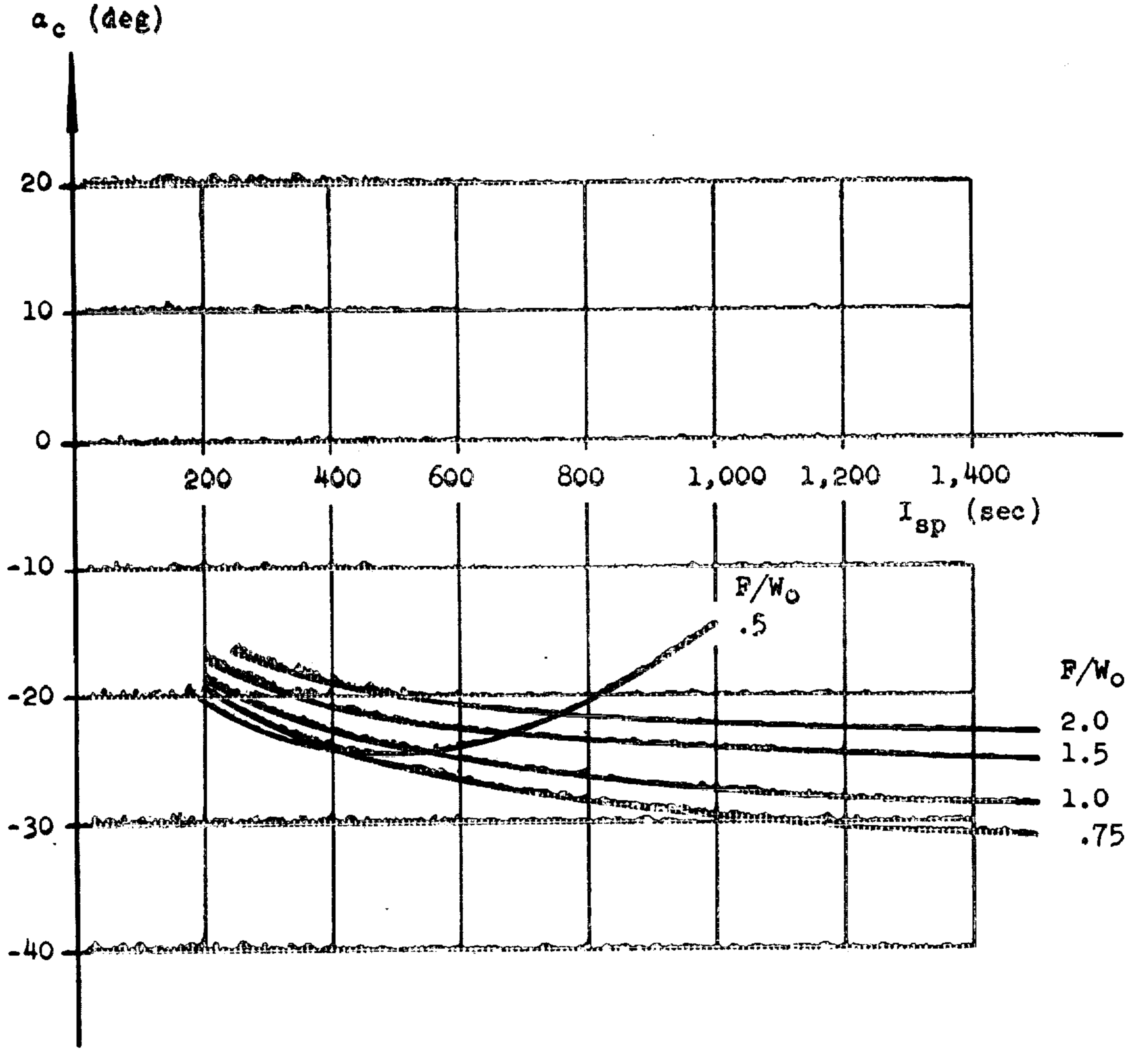

Angle at Cutoff for R_c = 100 km and Φ_I = 60°

FIGURE 3

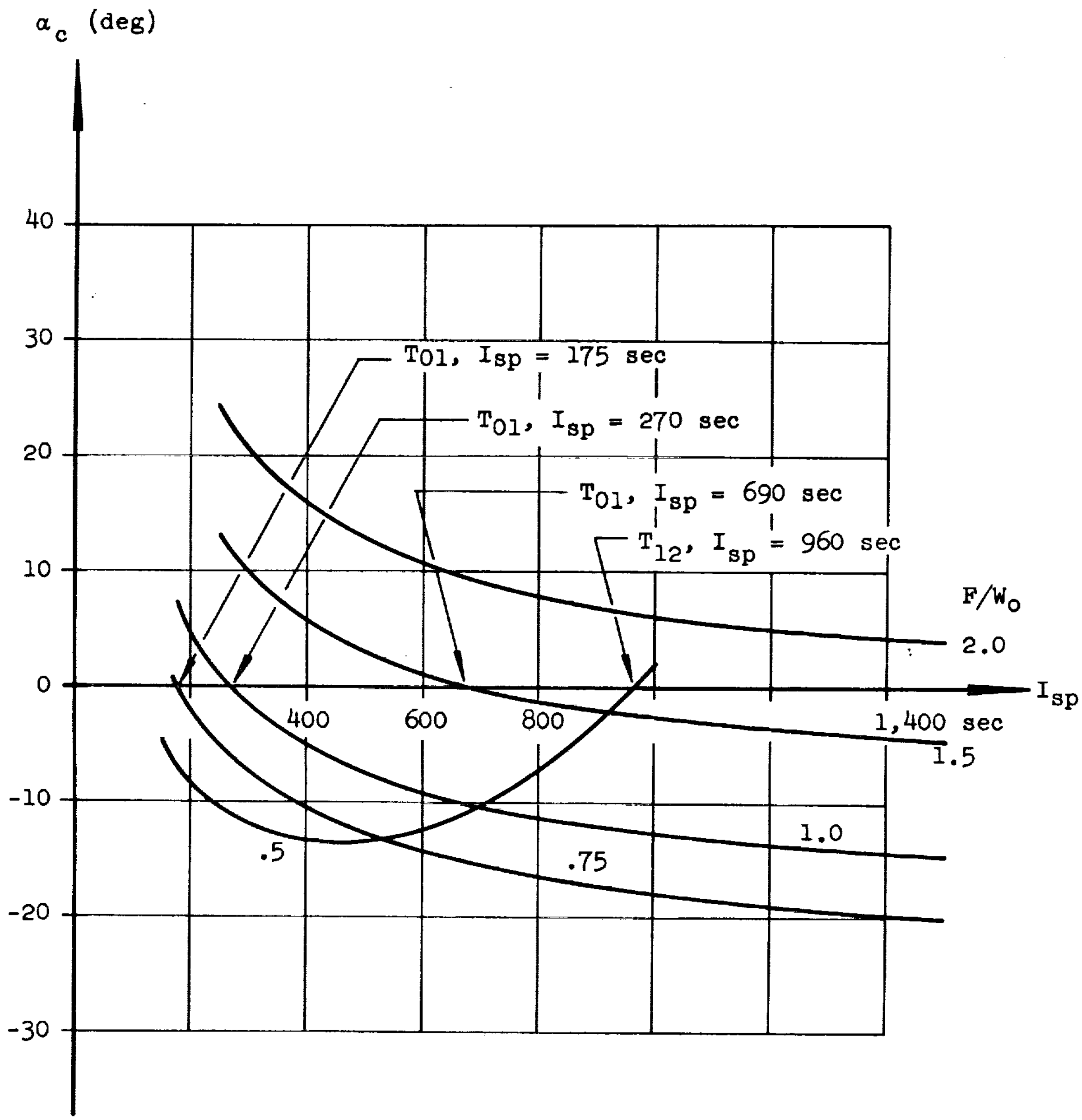

Angle at Cutoff for R_c = 200 km and ϕ_I = 60°

FIGURE 4

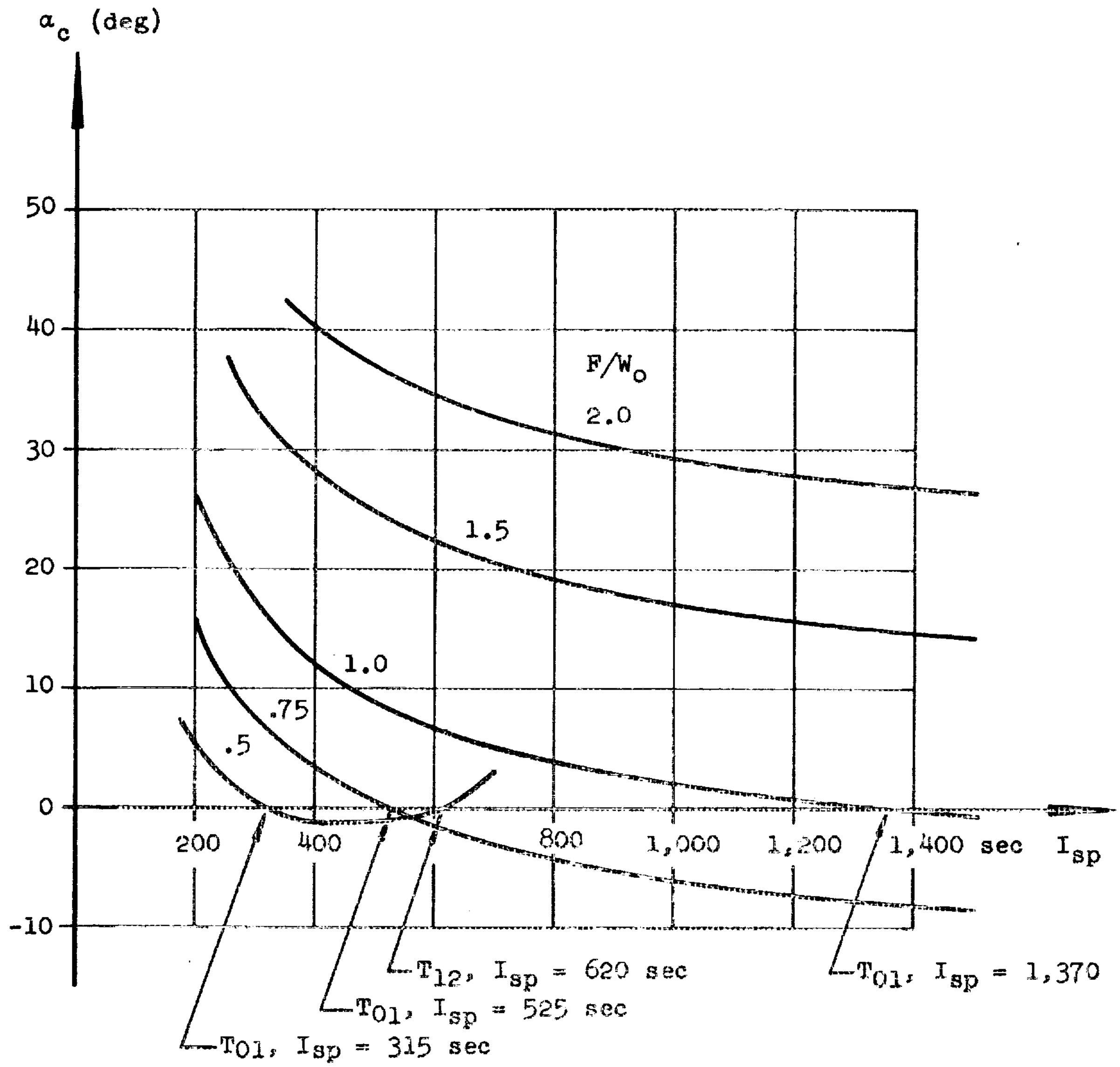

Angle at Cutoff for R_c = 300 km and Φ_I = 60°

FIGURE 5

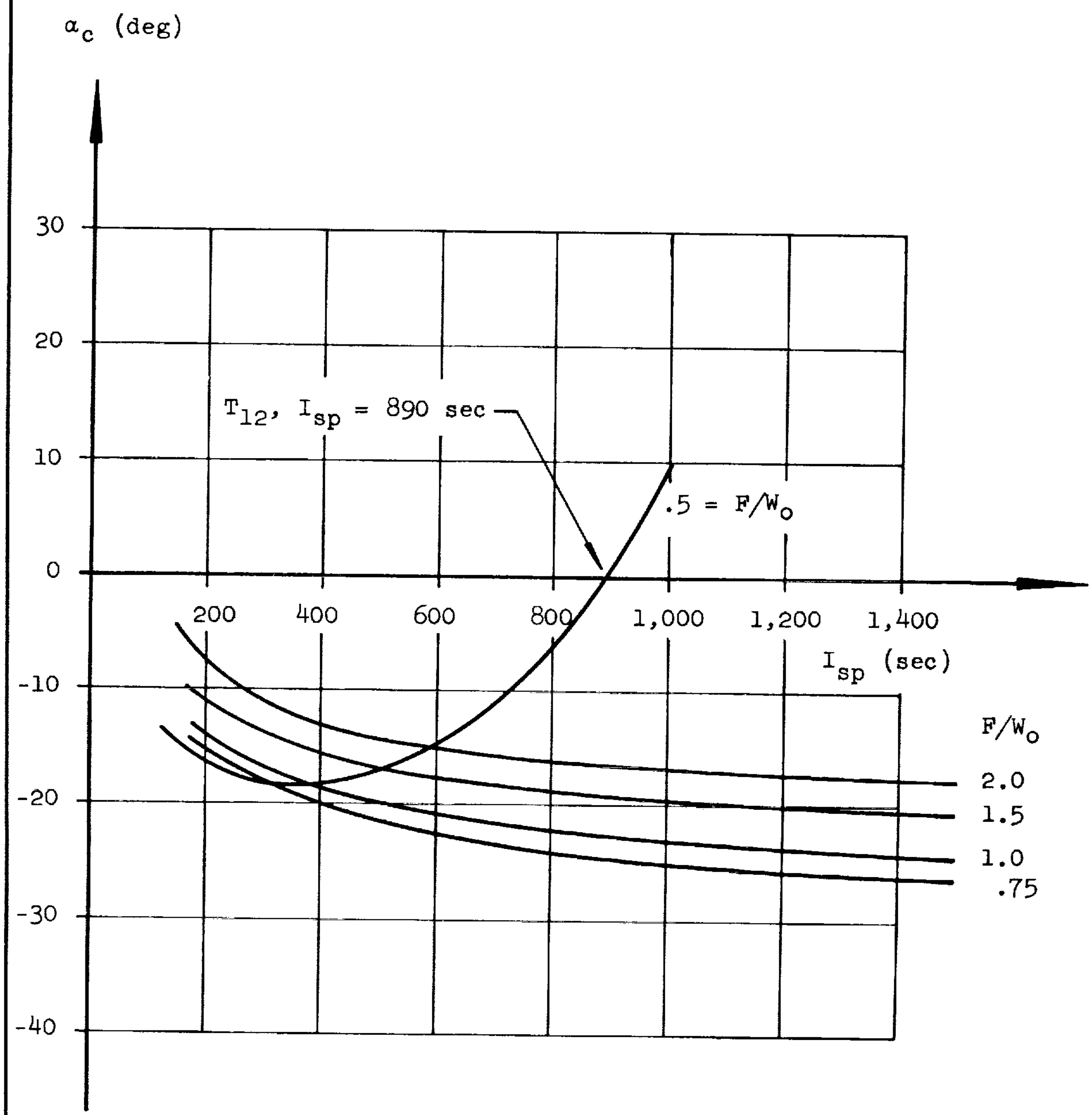

Angle at Cutoff for R_c = 100 km and $\vartheta_I = 65^o$

FIGURE 6

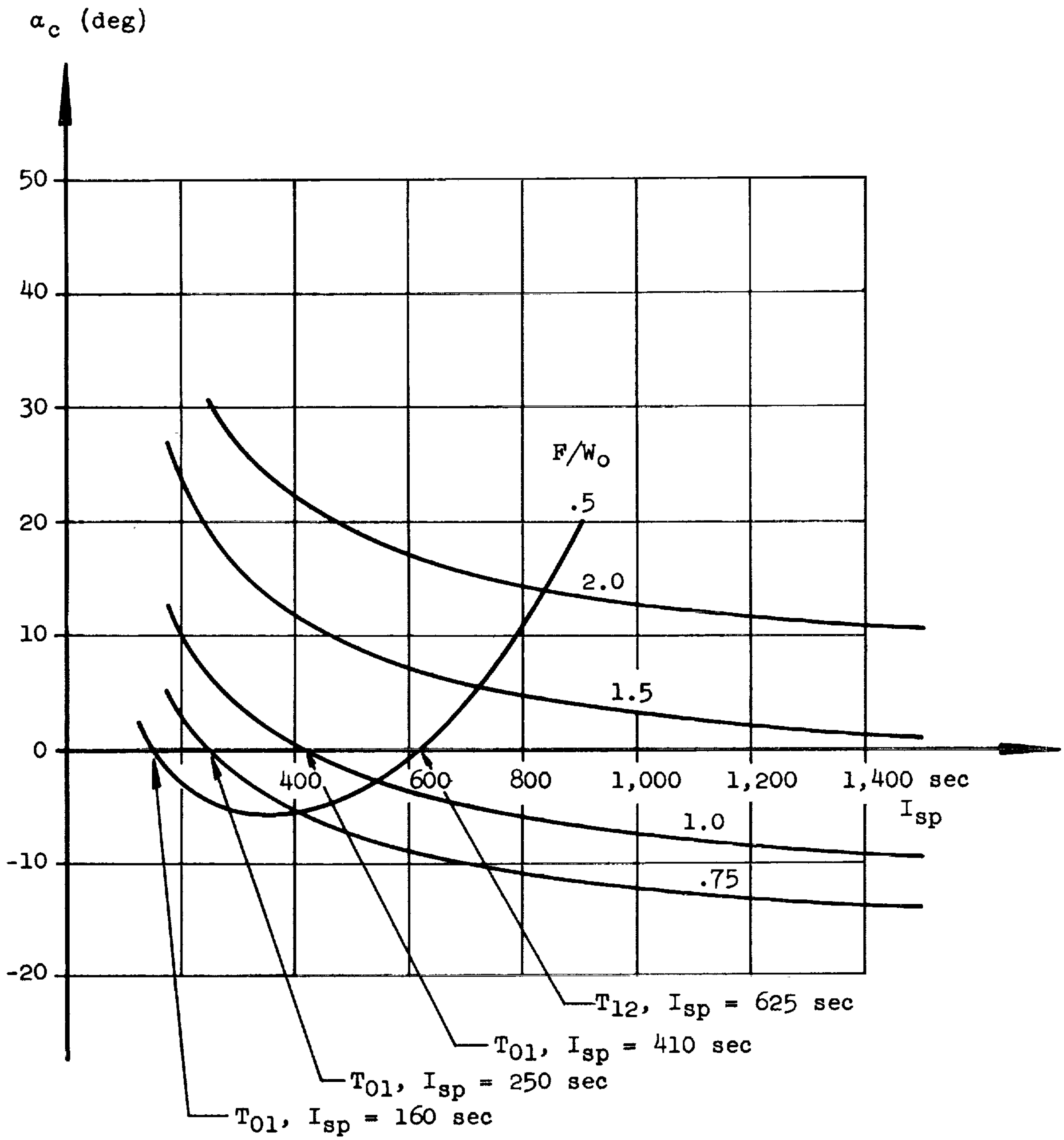

Angle at Cutoff for R_c = 200 km and $\Phi_I = 65^{\circ}$

FIGURE 7

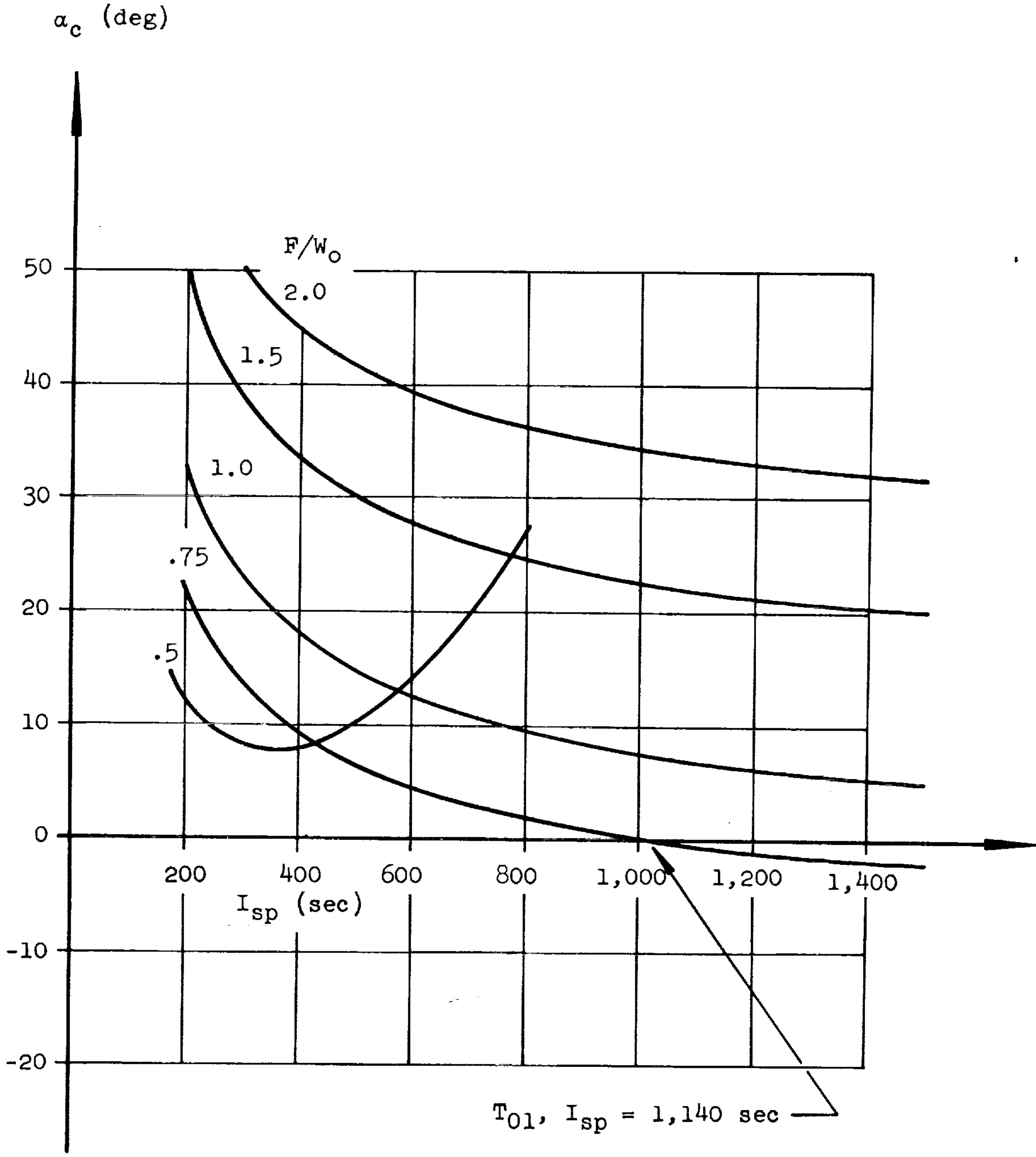

Angle at Cutoff for R_c = 300 km and ϑ_I = 65°

FIGURE 8

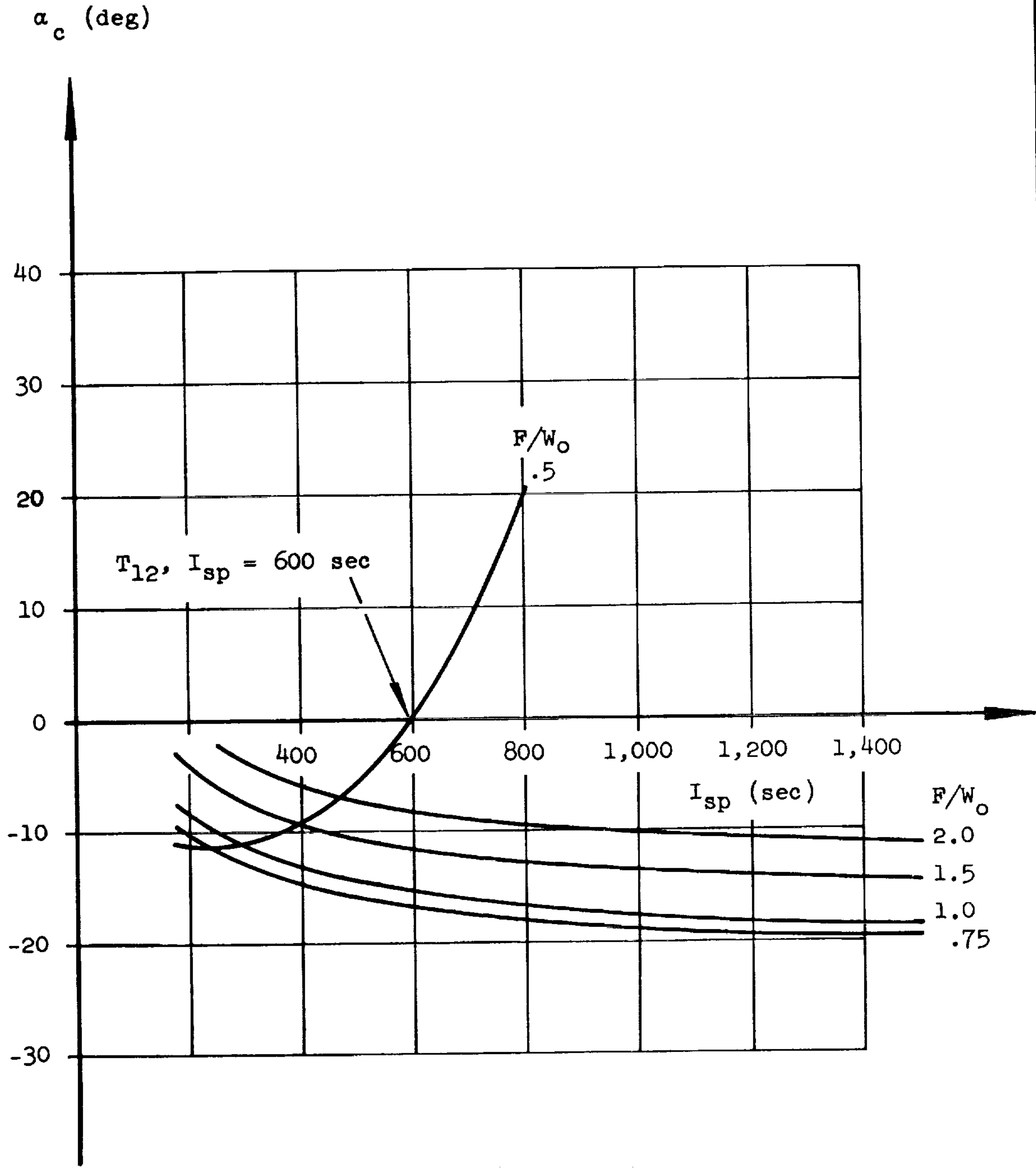

Angle at Cutoff for R_c = 100 km, $\$_I = 70^\circ$

FIGURE 9

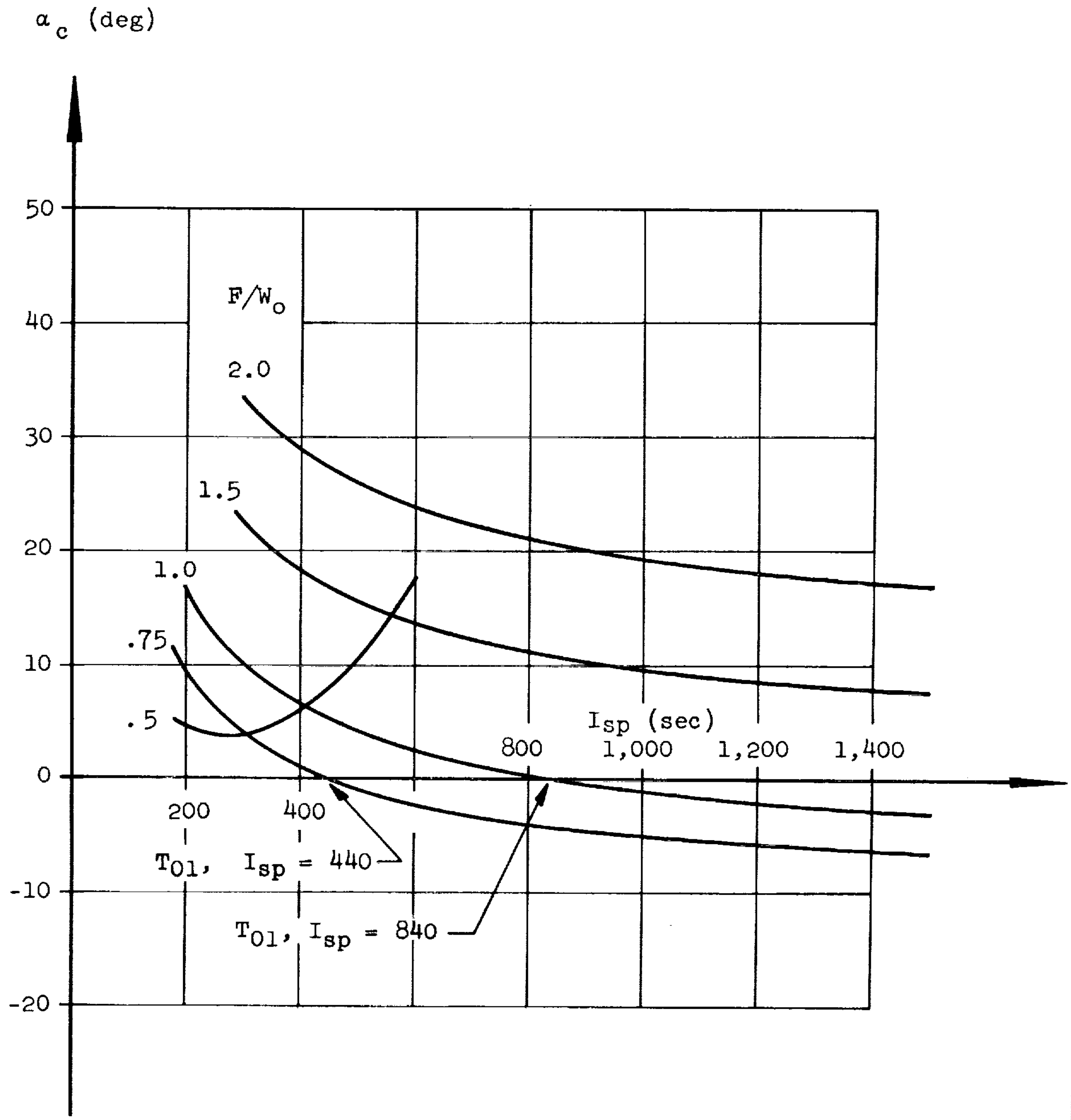

Angle at Cutoff for R_c = 200 km and $\phi_I = 70^\circ$

FIGURE 10

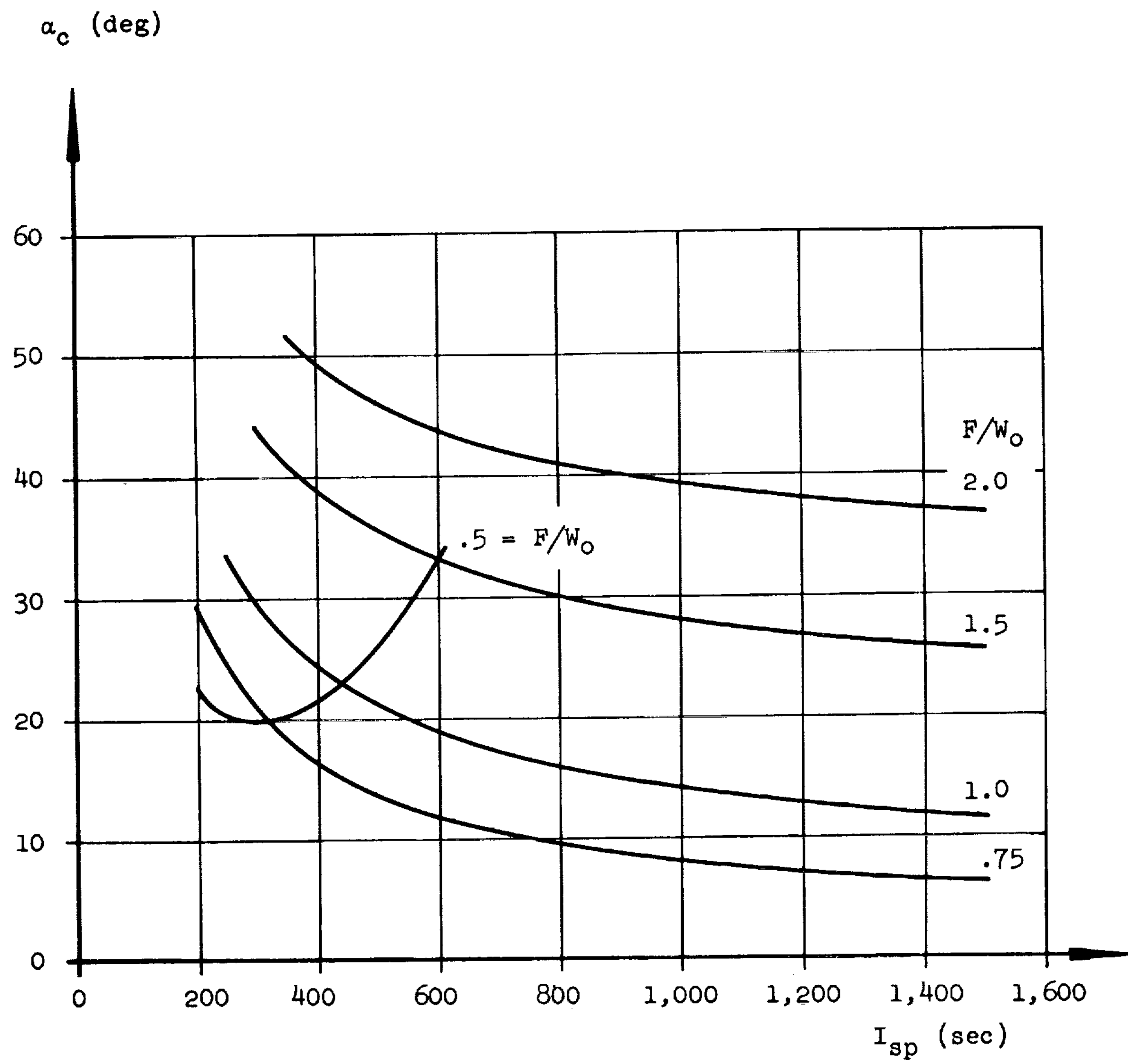

Angle at Cutoff for R_c = 300 km and $\Phi_I = 70^\circ$

FIGURE 11

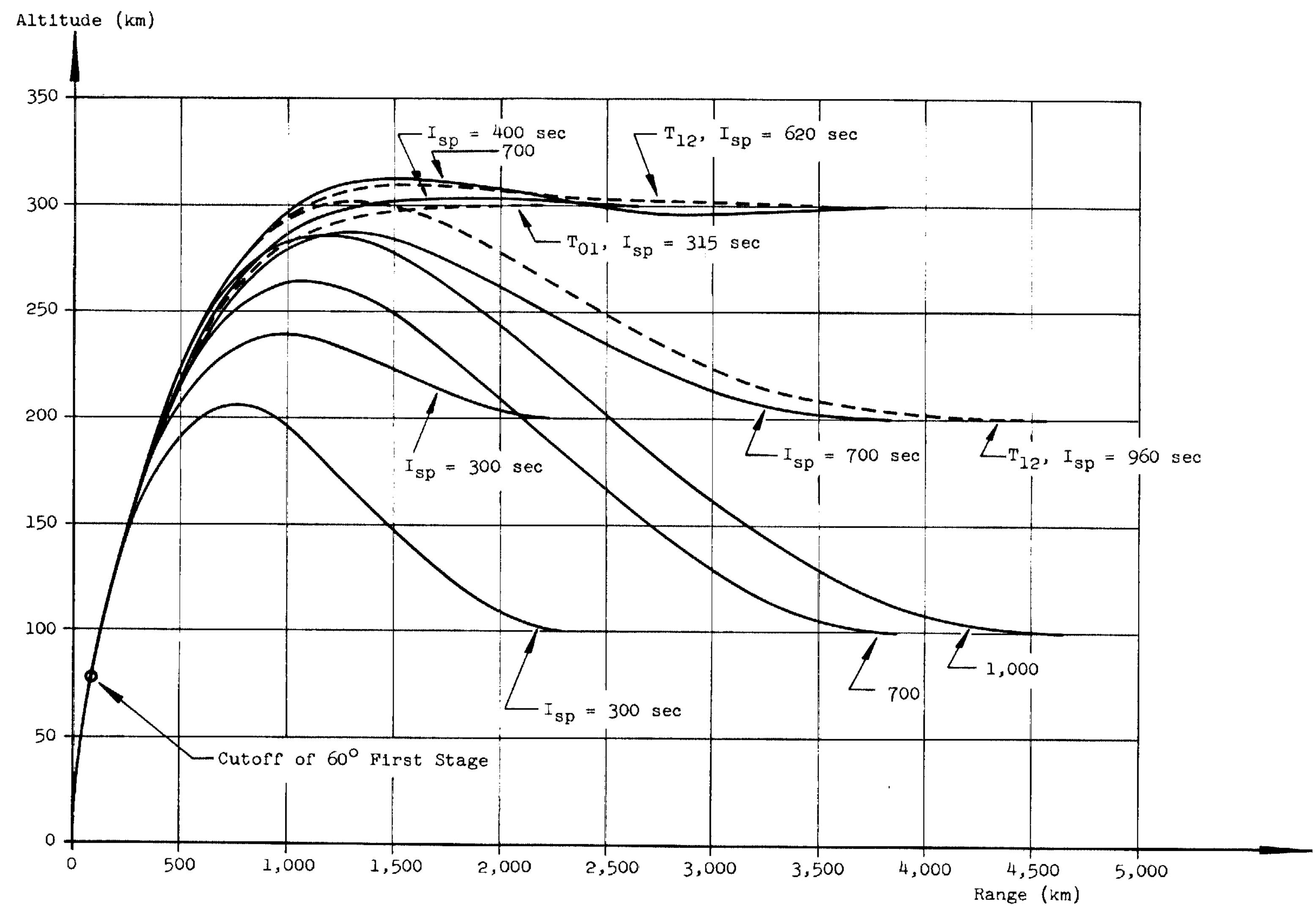

Trajectory Shapes for $F/W_o = .5$ and $\vartheta_I = 60^\circ$

FIGURE 12

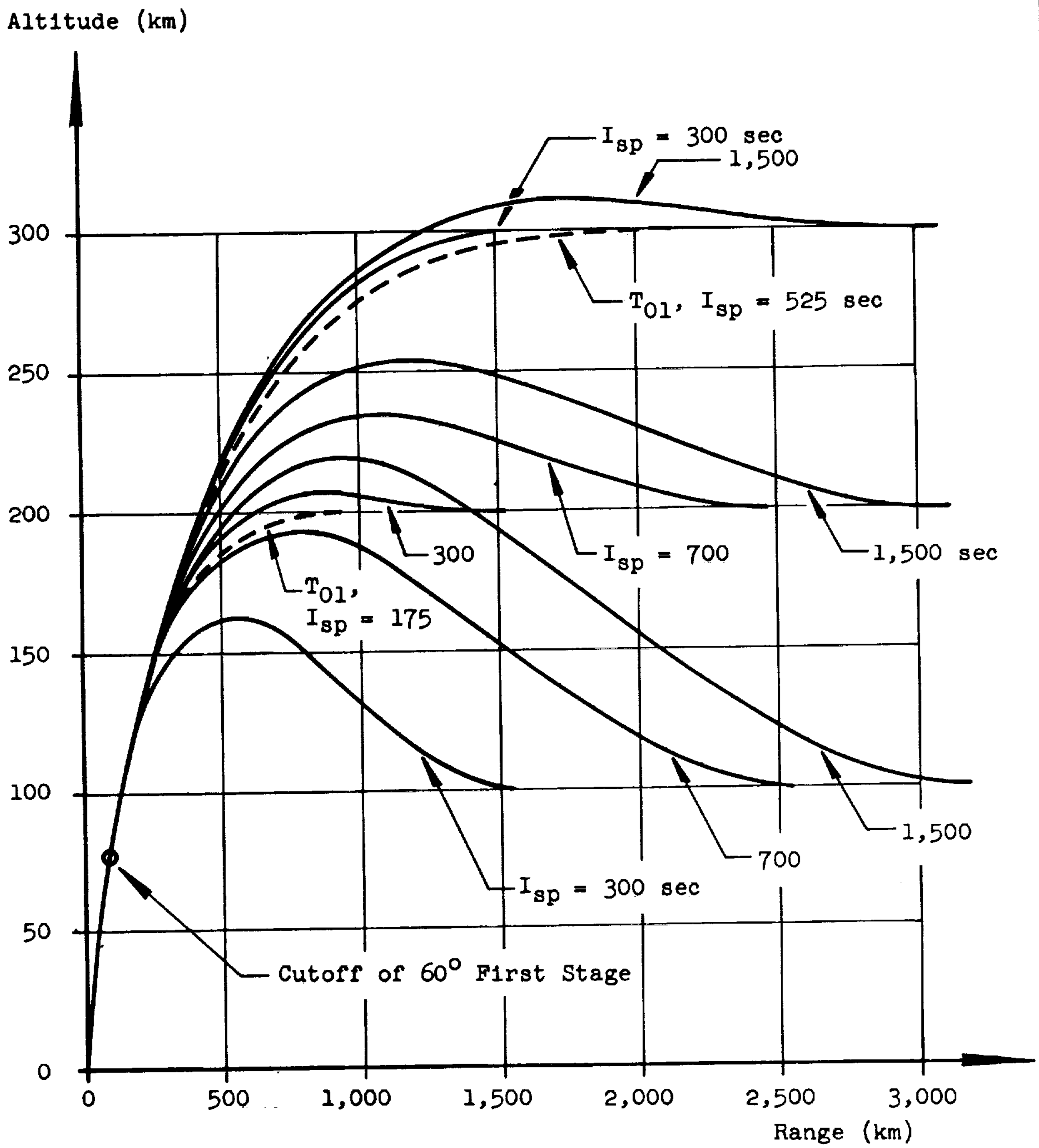

Trajectory Shapes for $F/W_0 = .75$ and $\vartheta_I = 60^\circ$

FIGURE 13

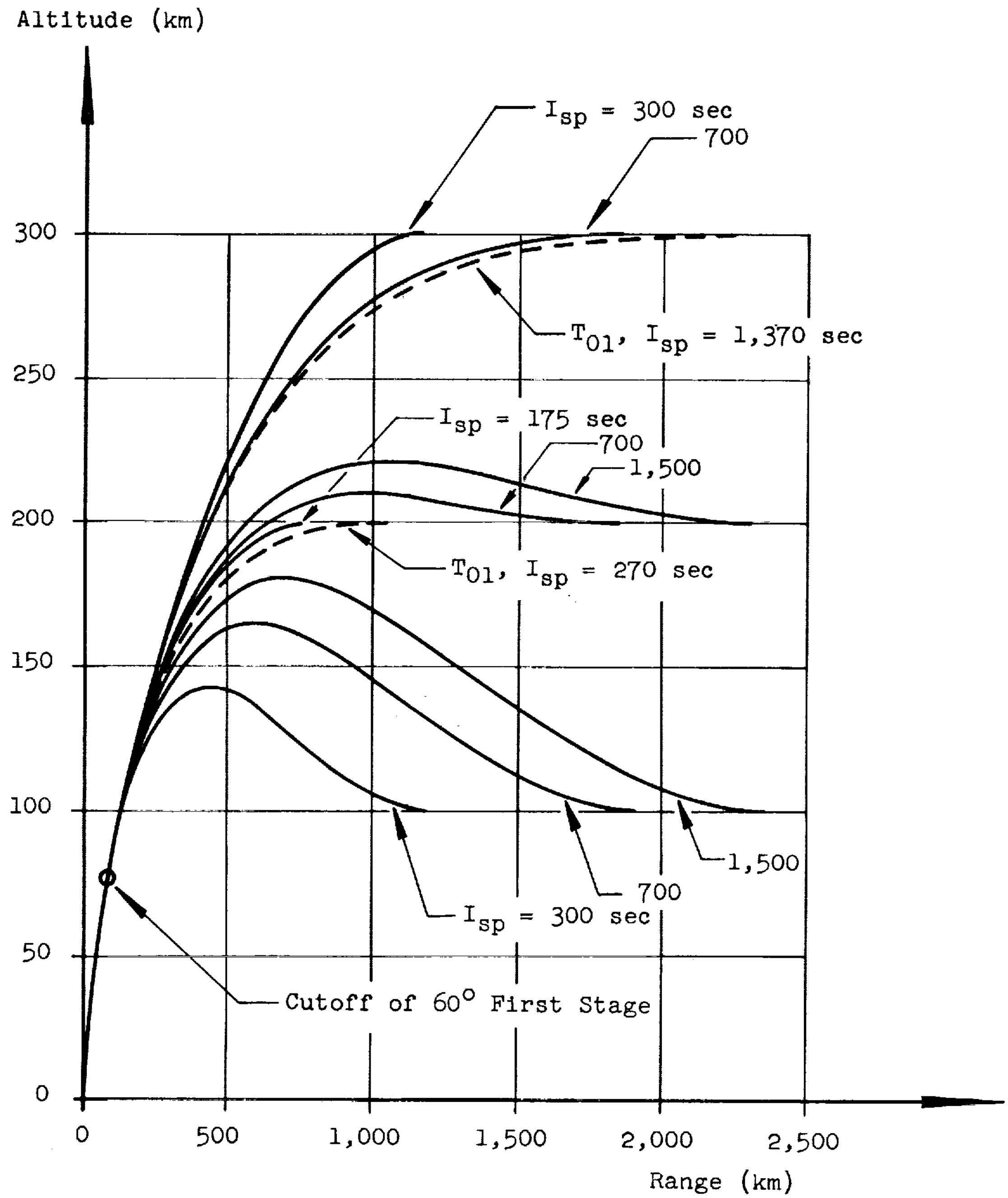

Trajectory Shapes for $F/W_o = 1.0$ and $\theta_I = 60^o$

FIGURE 14

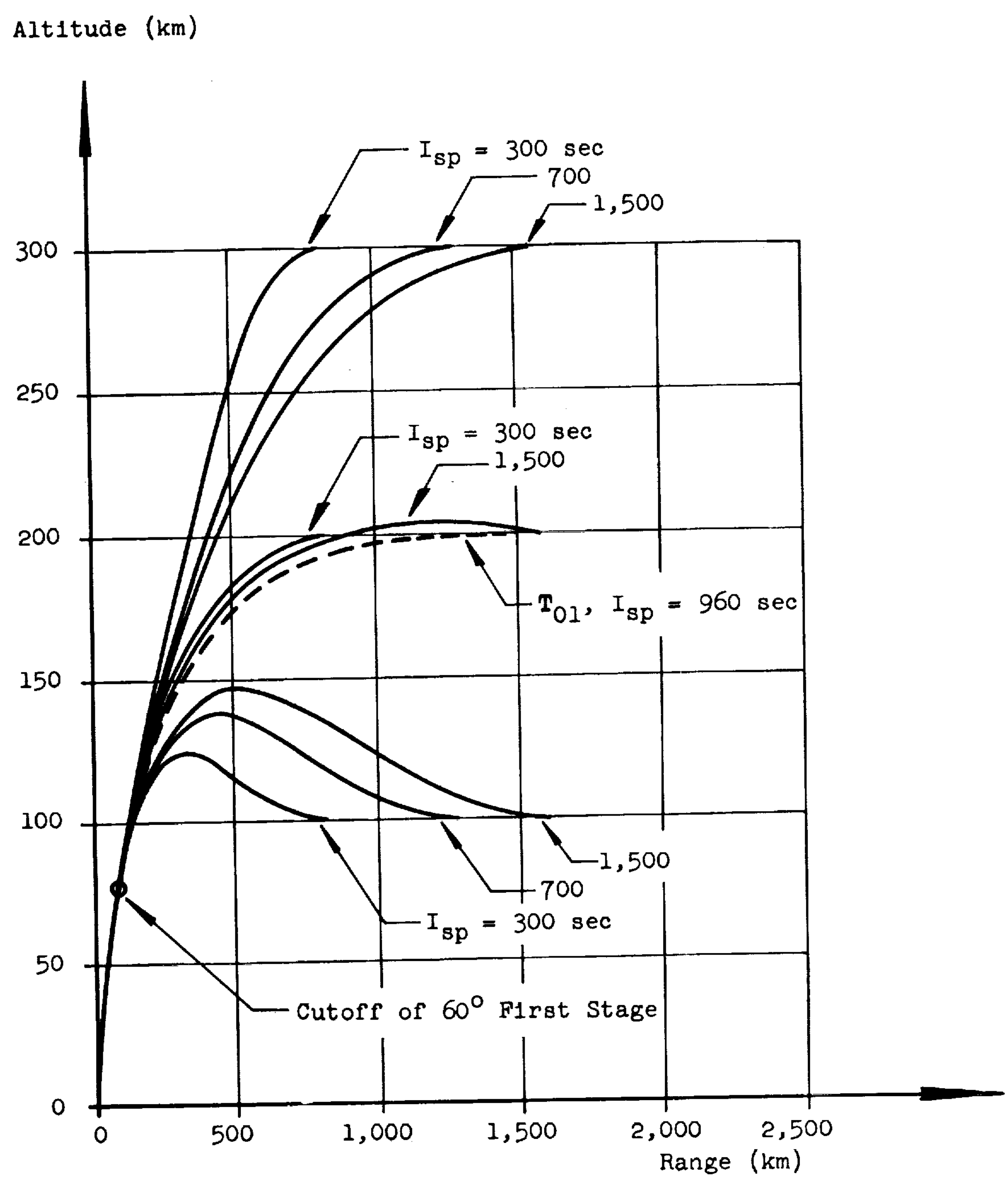

Trajectory Shapes for $F/W_o = 1.5$ and $\phi_I = 60^o$

FIGURE 15

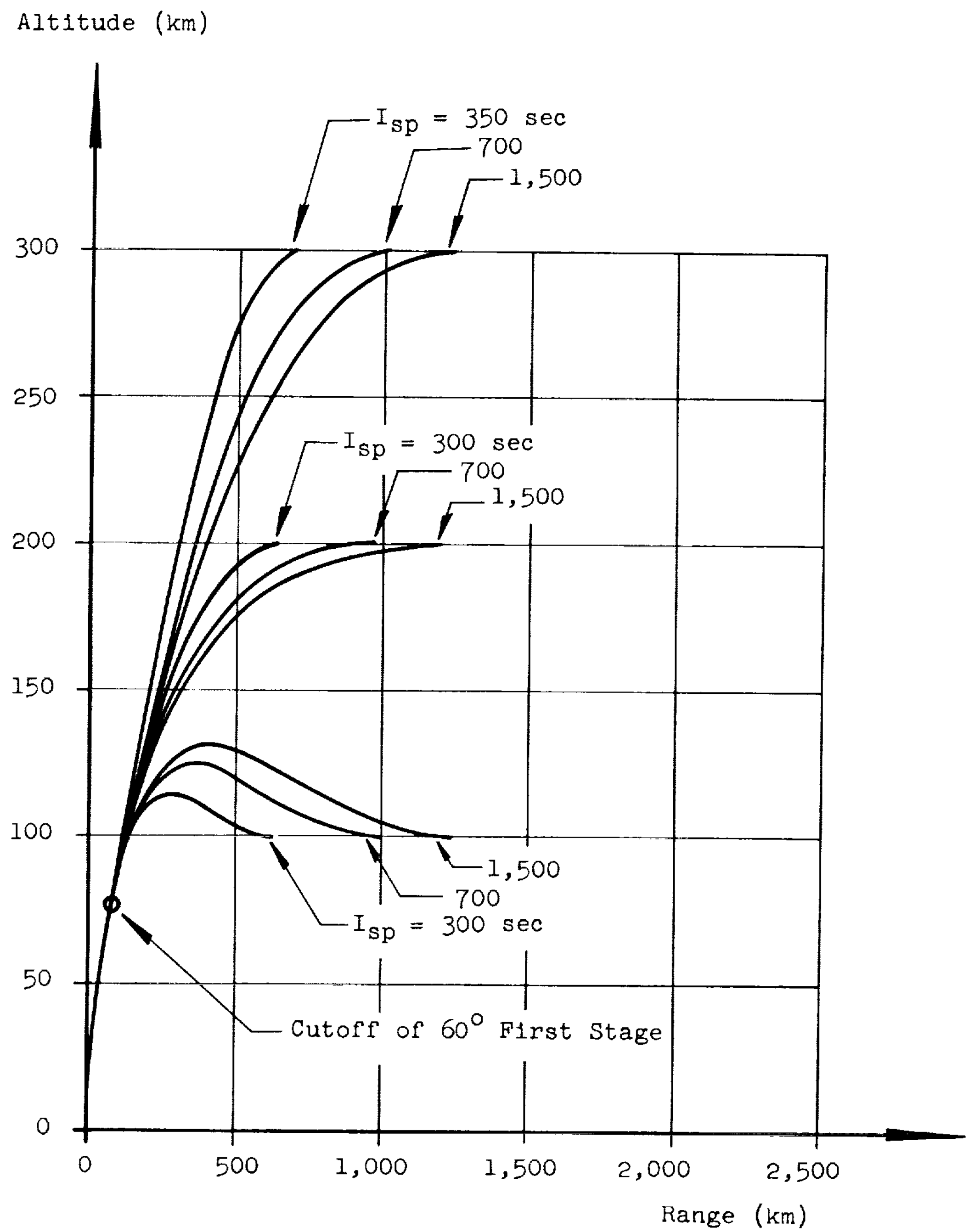

Trajectory Shapes for $F/W_o = 2.0$ and $\vartheta_I = 60^\circ$

FIGURE 16

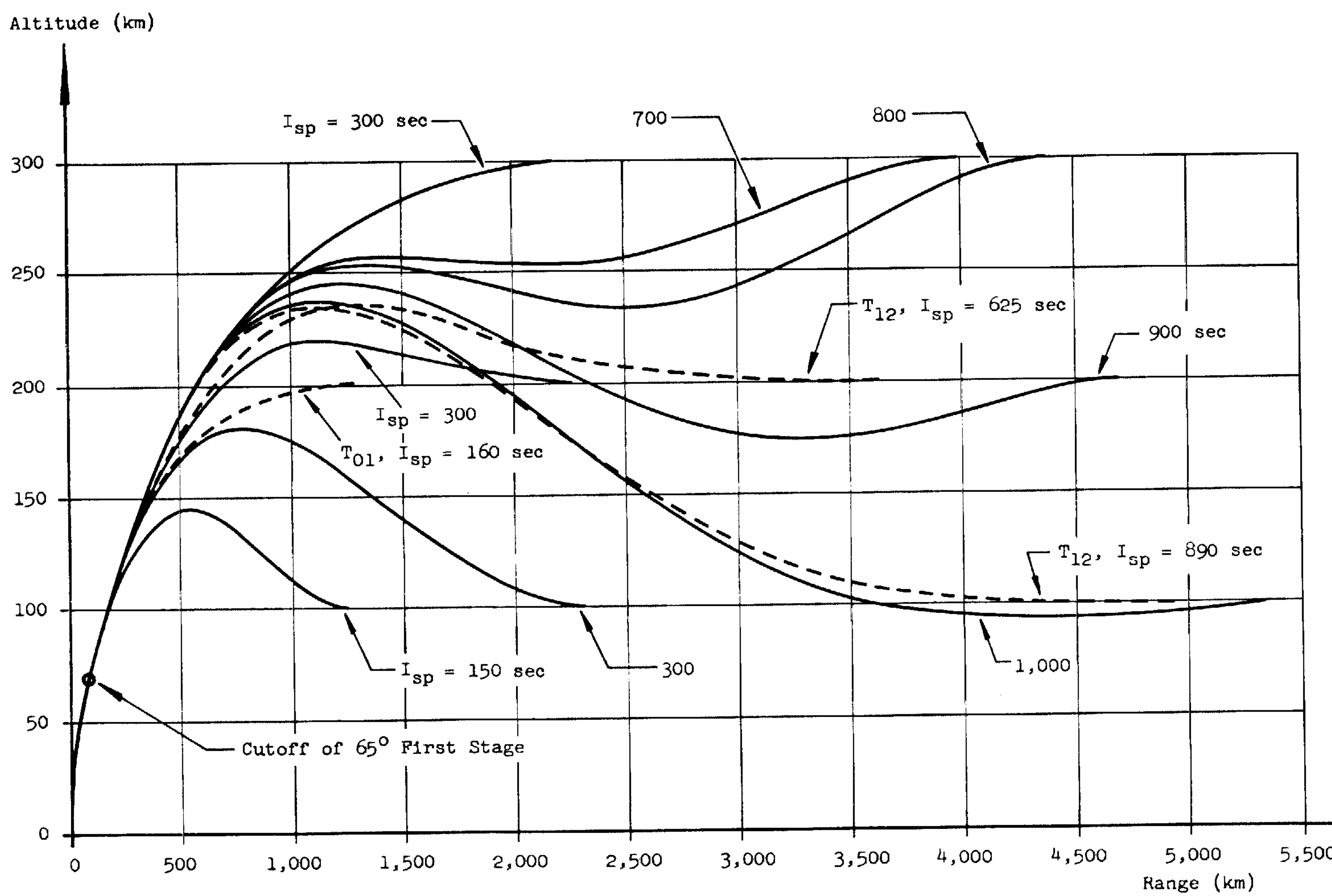

Trajectory Shapes for $F/W_o = .5$ and $\psi_I = 65^\circ$

FIGURE 17

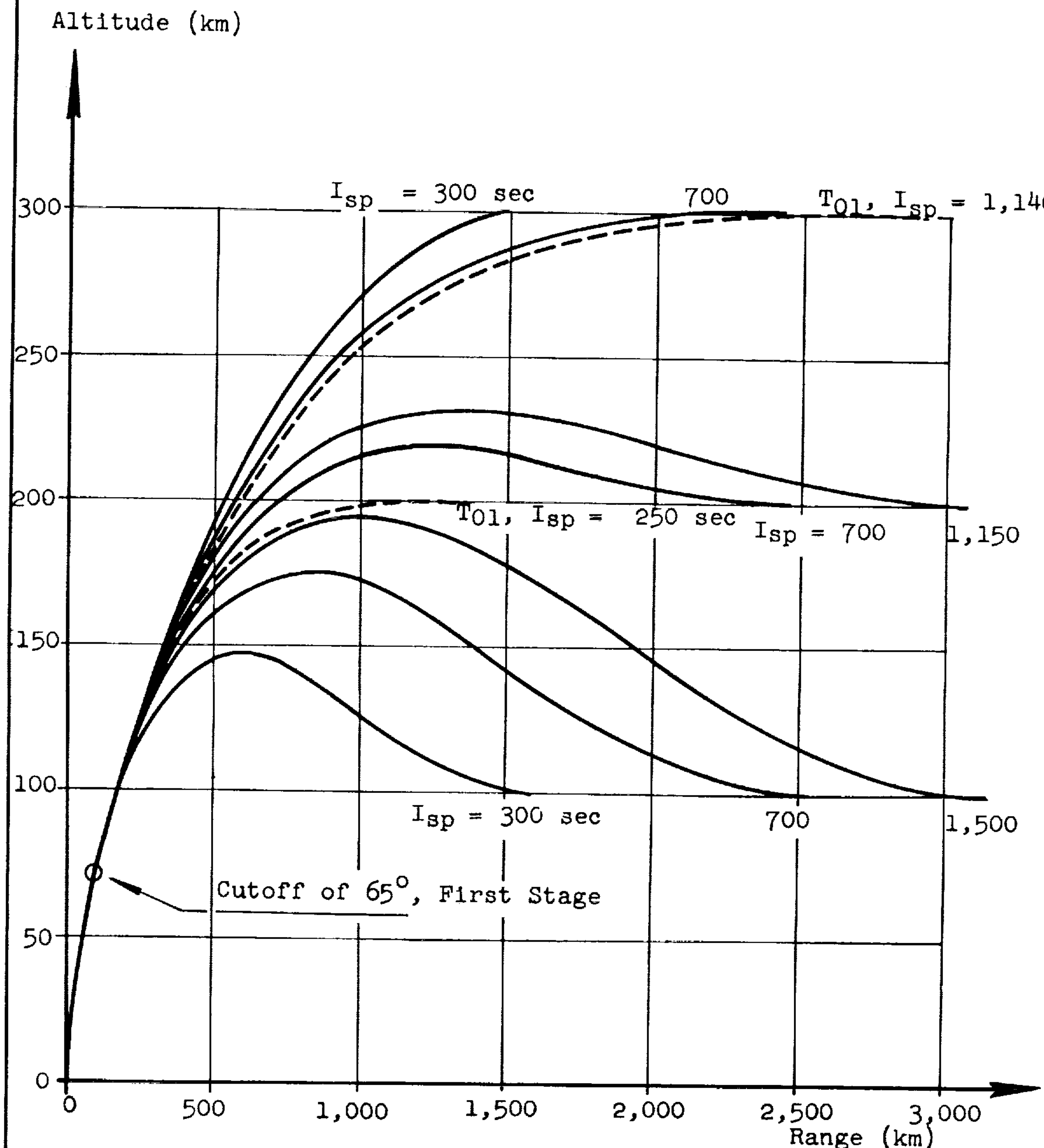

TRAJECTORY SHAPES FOR F/W_o = .75 AND ϑ_I = 65 DEG

FIGURE 18

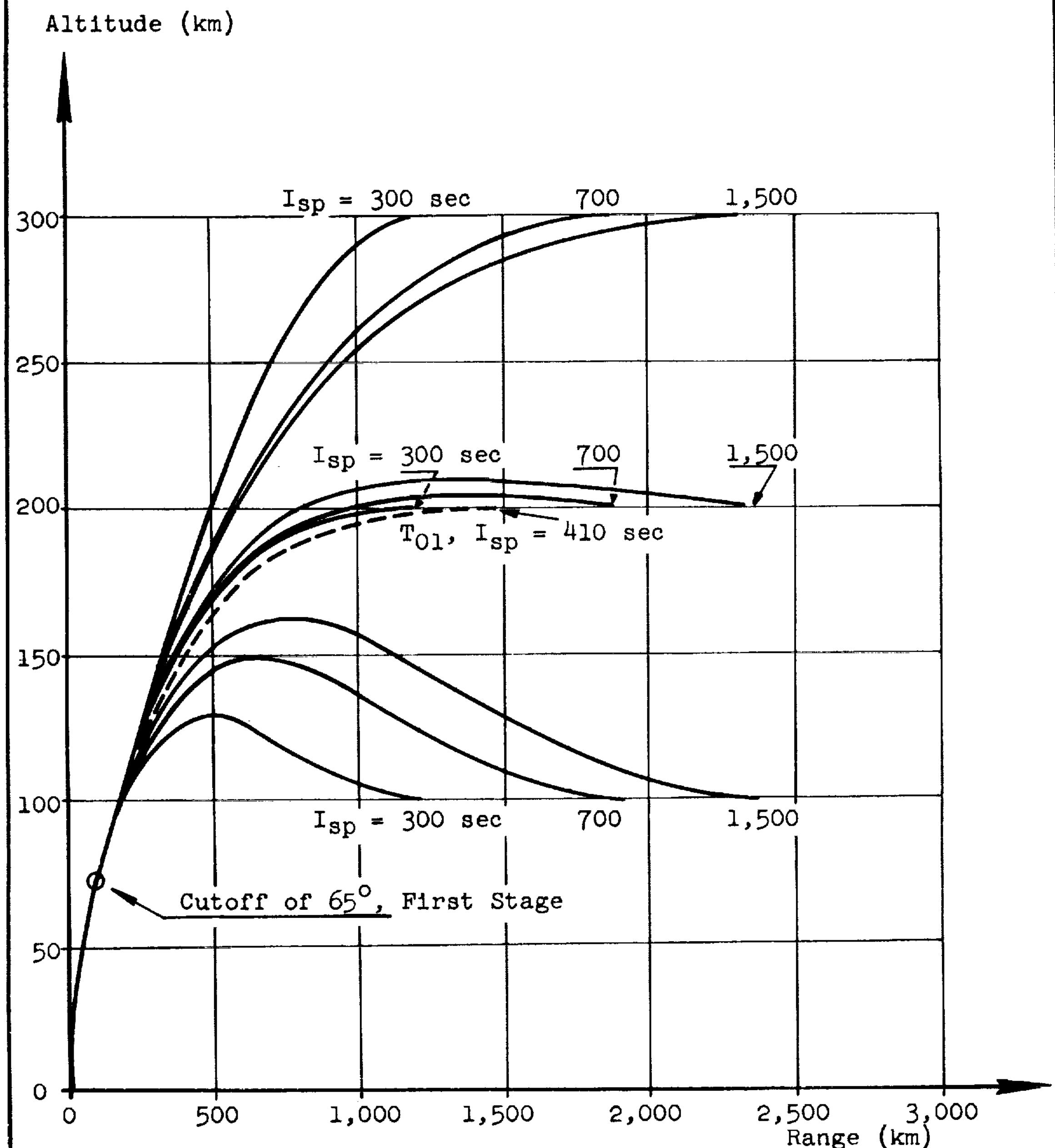

TRAJECTORY SHAPES FOR F/W_o = 1.0 AND ϑ_I = 65 DEG

FIGURE 19

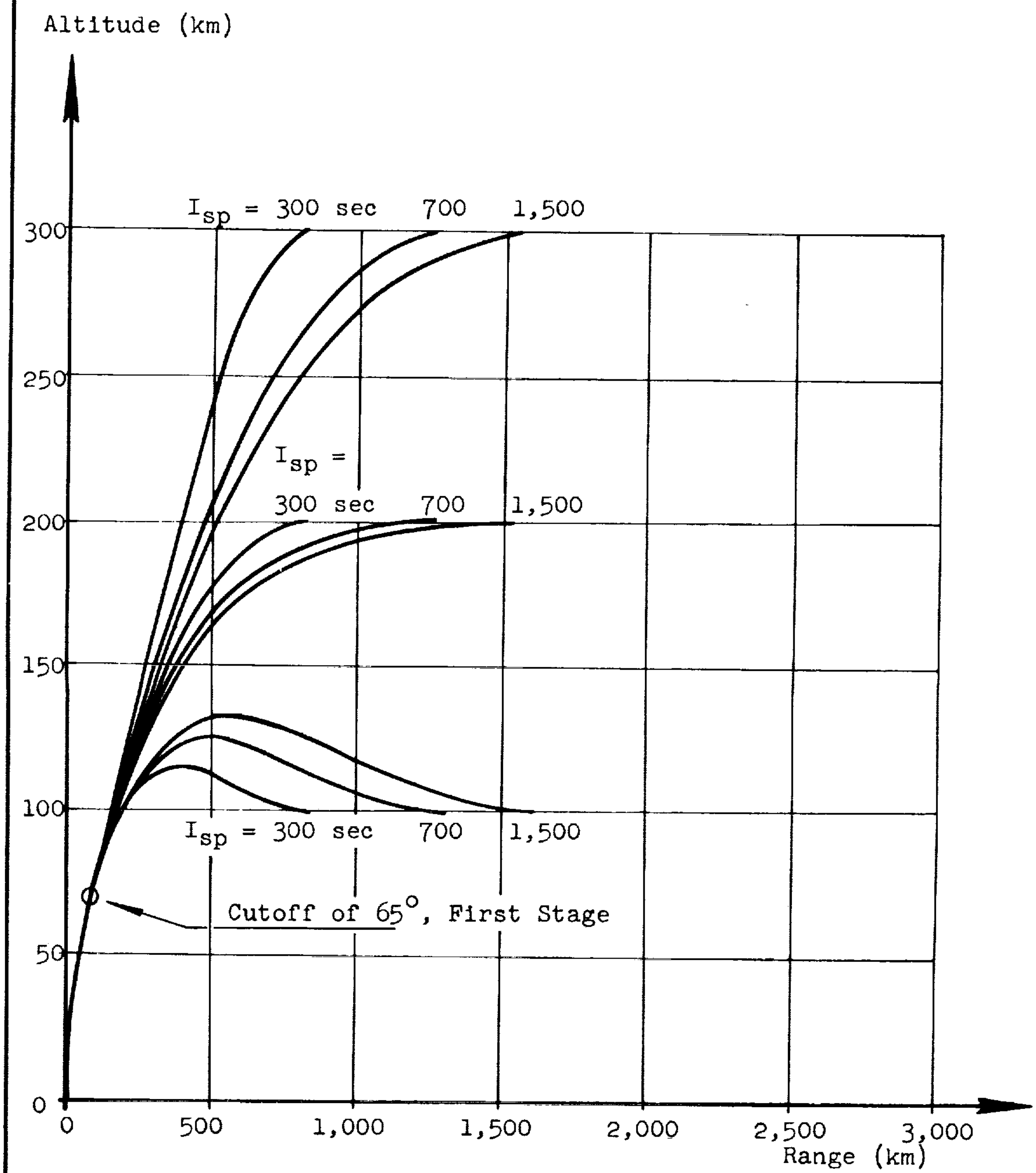

TRAJECTORY SHAPES FOR $F/W_o = 1.5$ AND $\vartheta_I = 65$ DEG

FIGURE 20

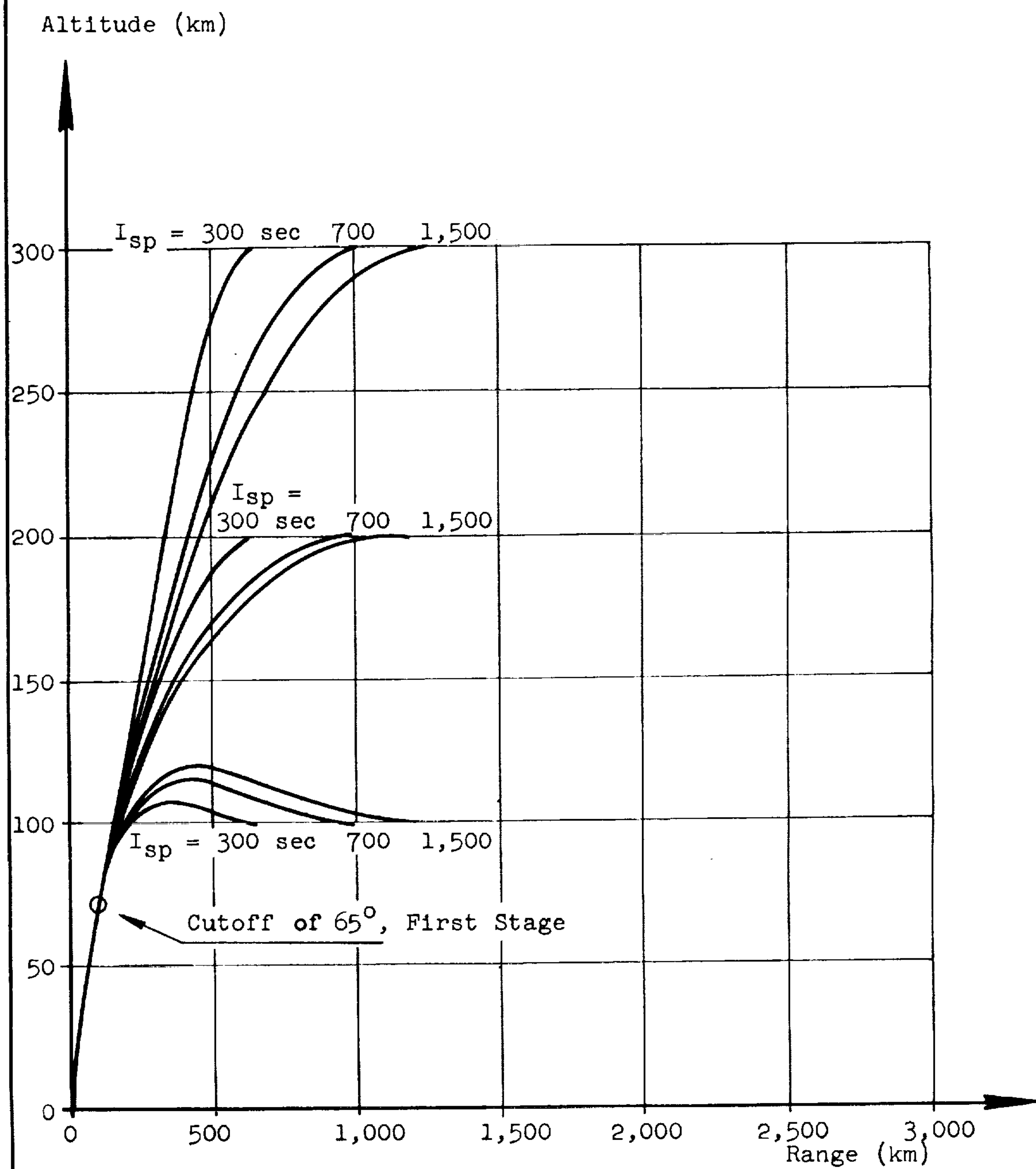

TRAJECTORY SHAPES FOR F/W_o = 2.0 AND ϑ_I = 65 DEG

FIGURE 21

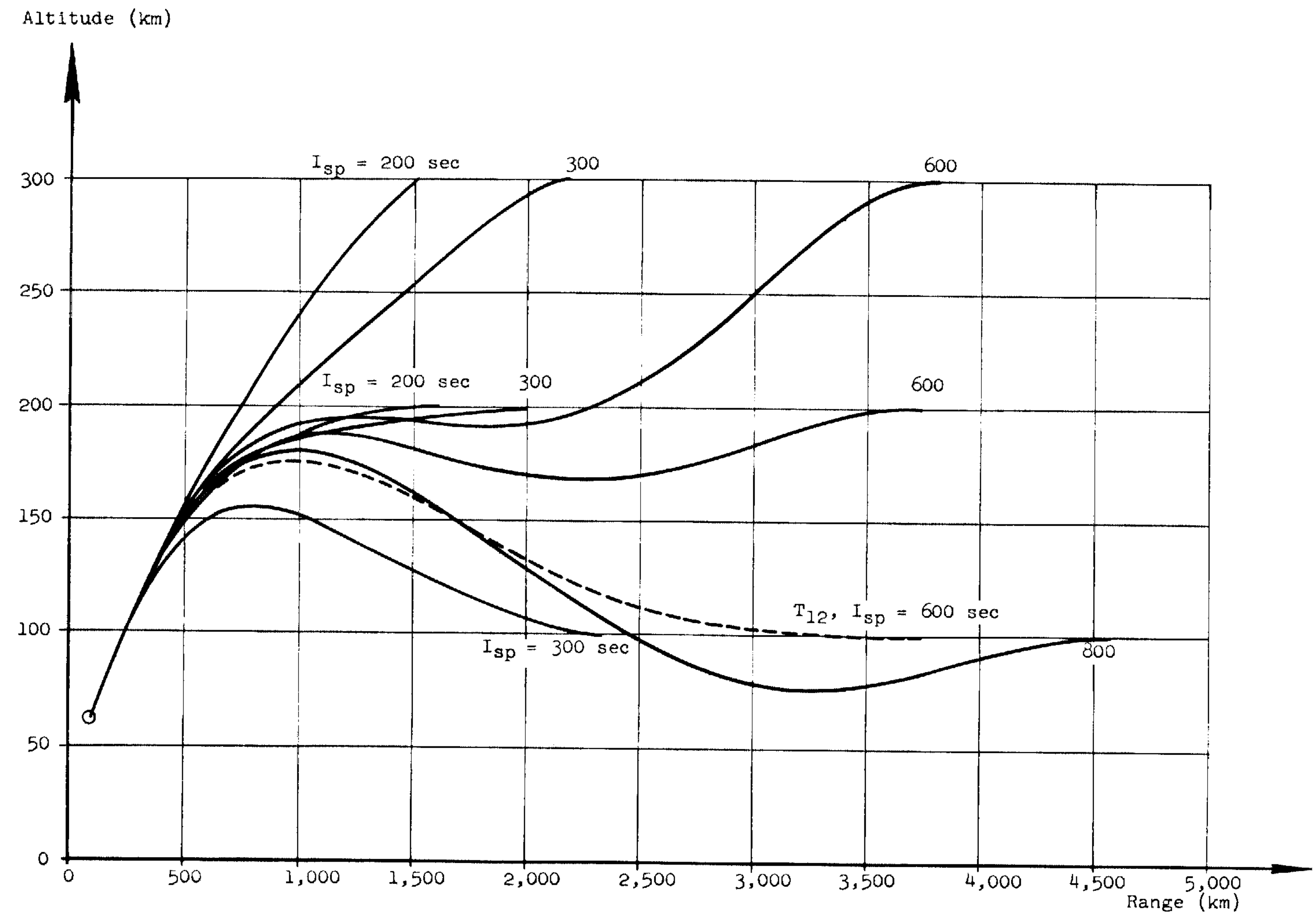

TRAJECTORY SHAPES FOR F/W_o = .5 AND $\$_I$ = 70 DEG

FIGURE 22

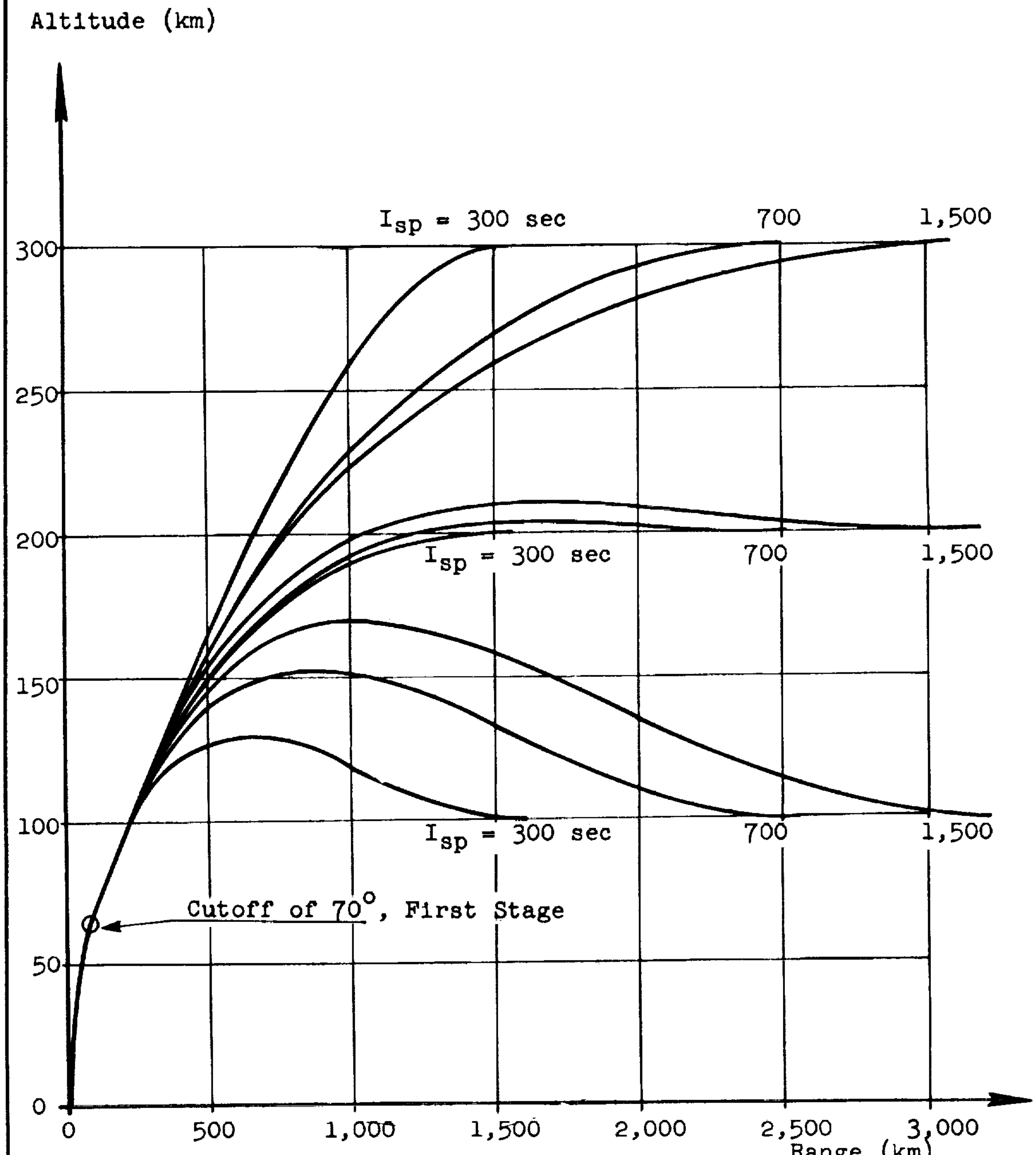

TRAJECTORY SHAPES FOR F/W_o = .75 AND θ_I = 70 DEG

FIGURE 23

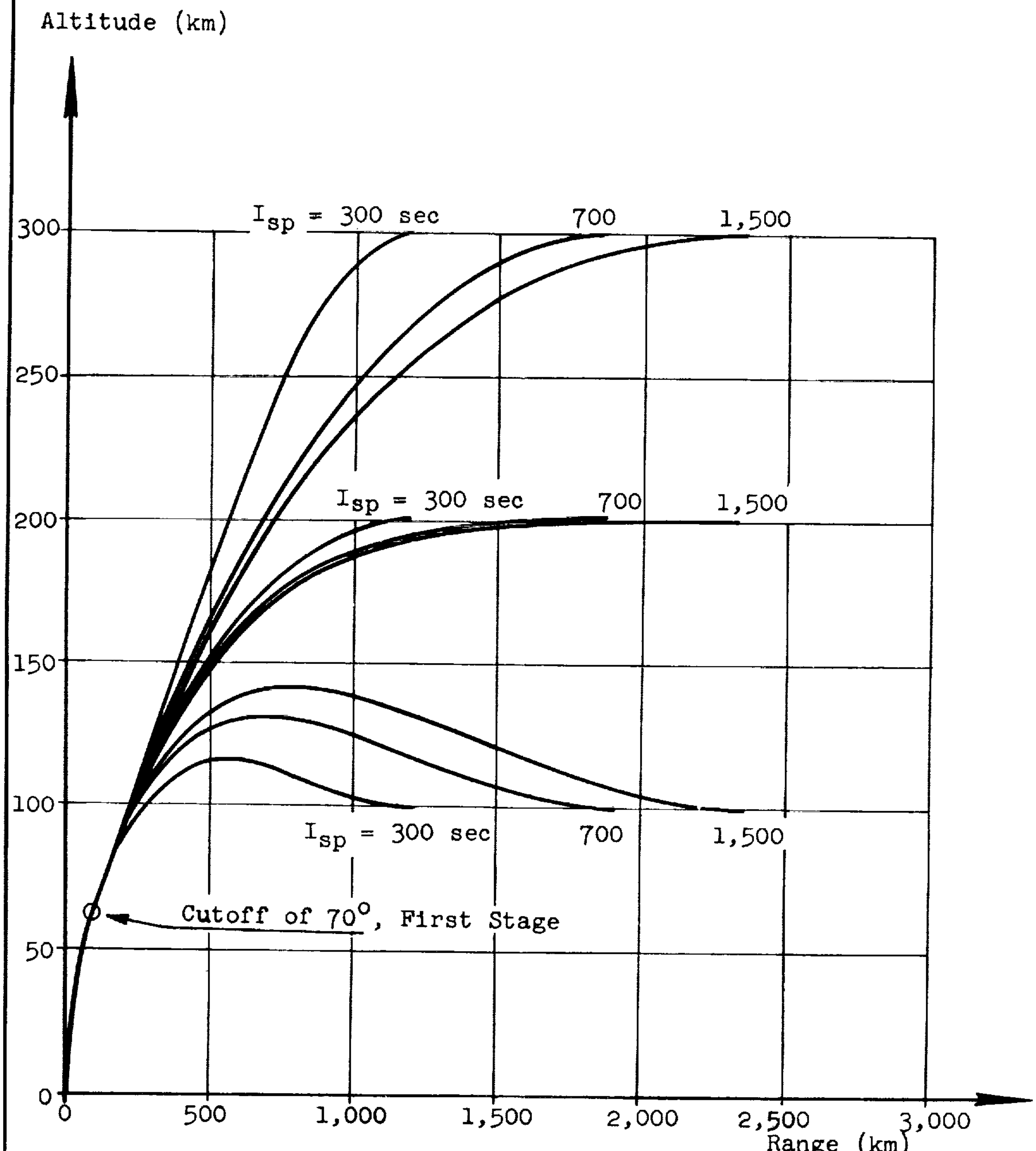

TRAJECTORY SHAPES FOR $F/W_o = 1.0$ AND $\vartheta_I = 70$ DEG

FIGURE 24

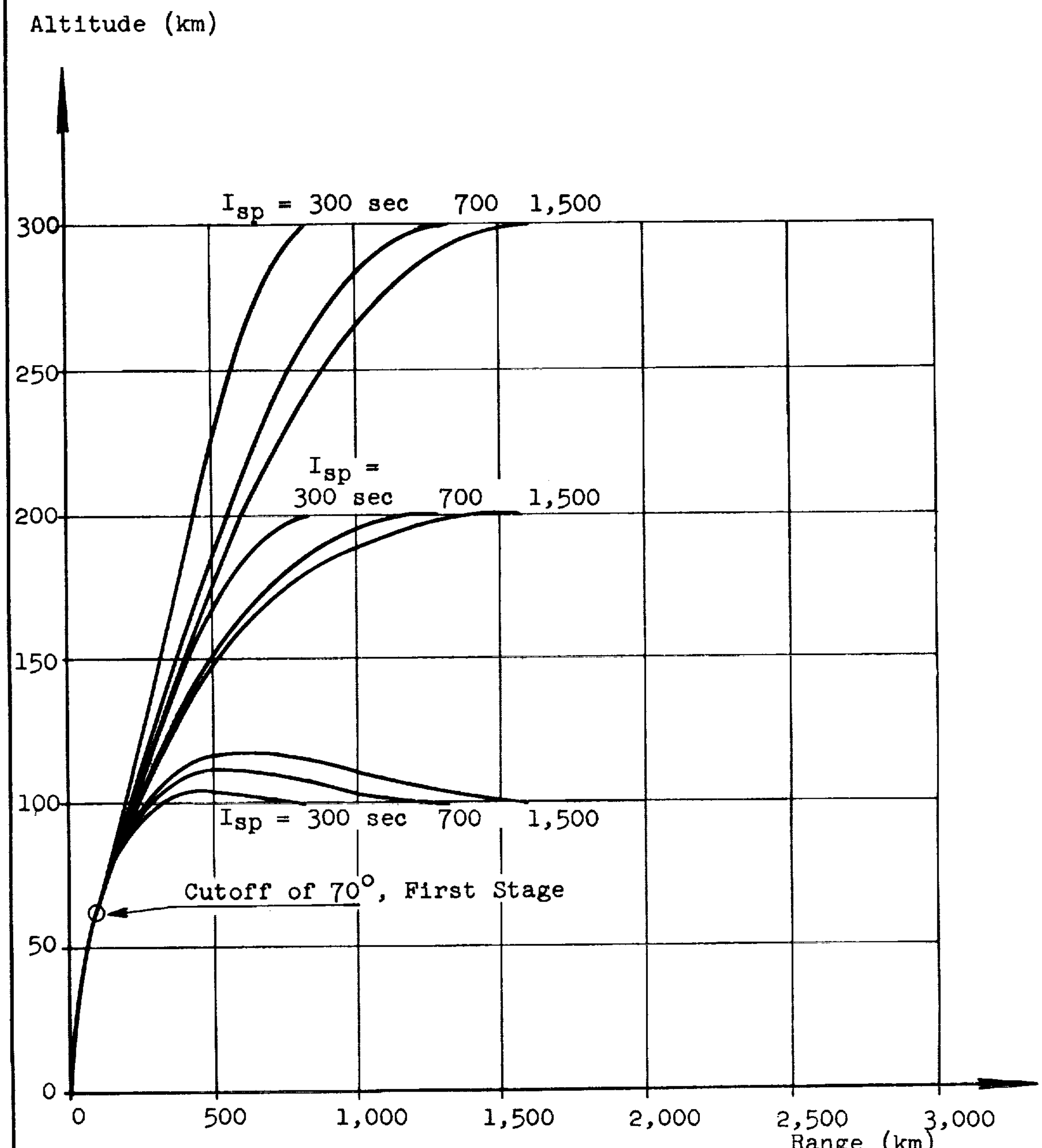

TRAJECTORY SHAPES FOR F/W_o = 1.5 AND ϑ_I = 70 DEG

FIGURE 25

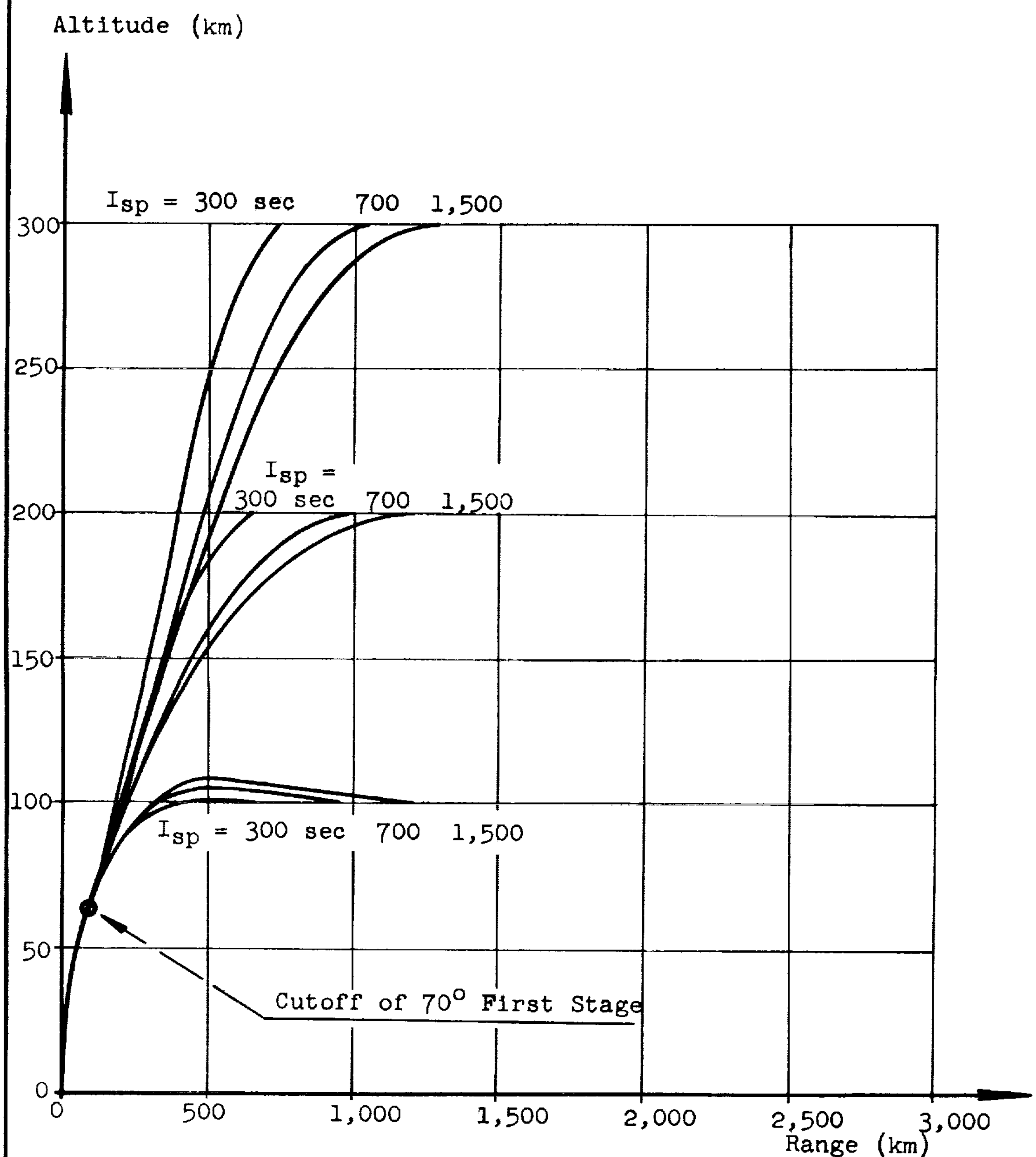

TRAJECTORY SHAPES FOR F/W_o = 2.0 AND ϑ_I = 70 DEG

FIGURE 26

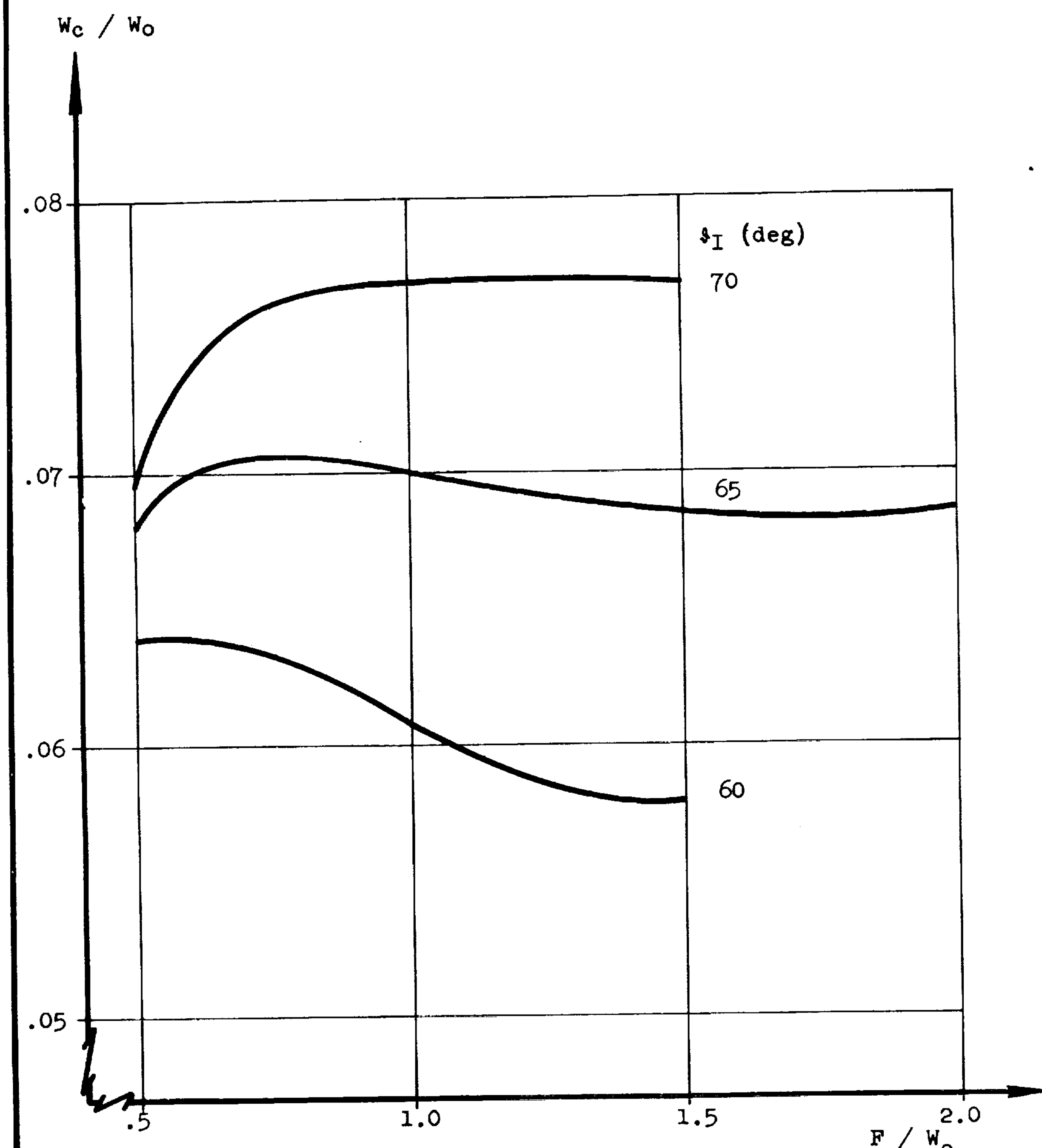

y_c = 100 km I_{sp} = 200 sec

FIGURE 27

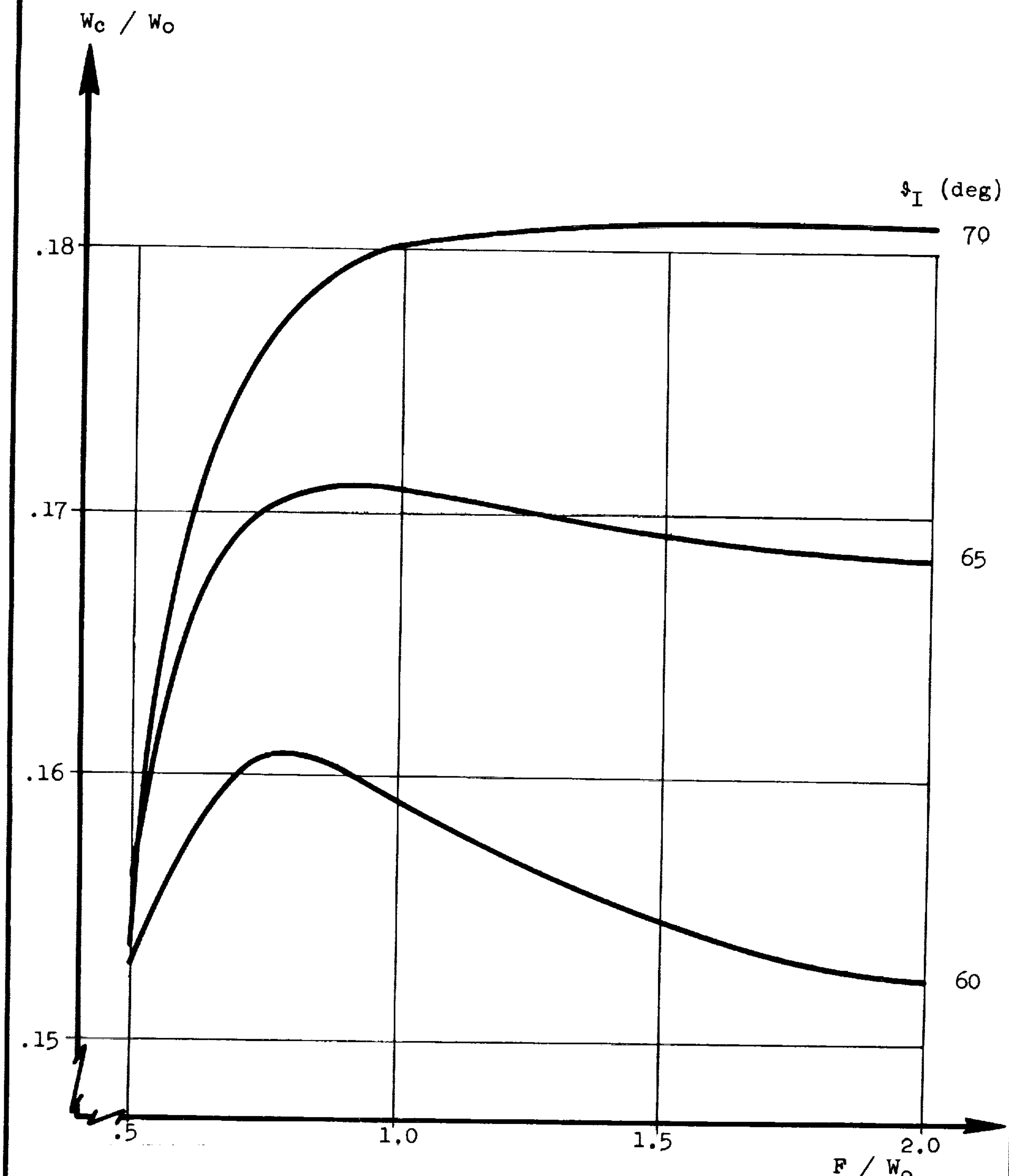

y_c = 100 km I_{sp} = 300 sec

FIGURE 28

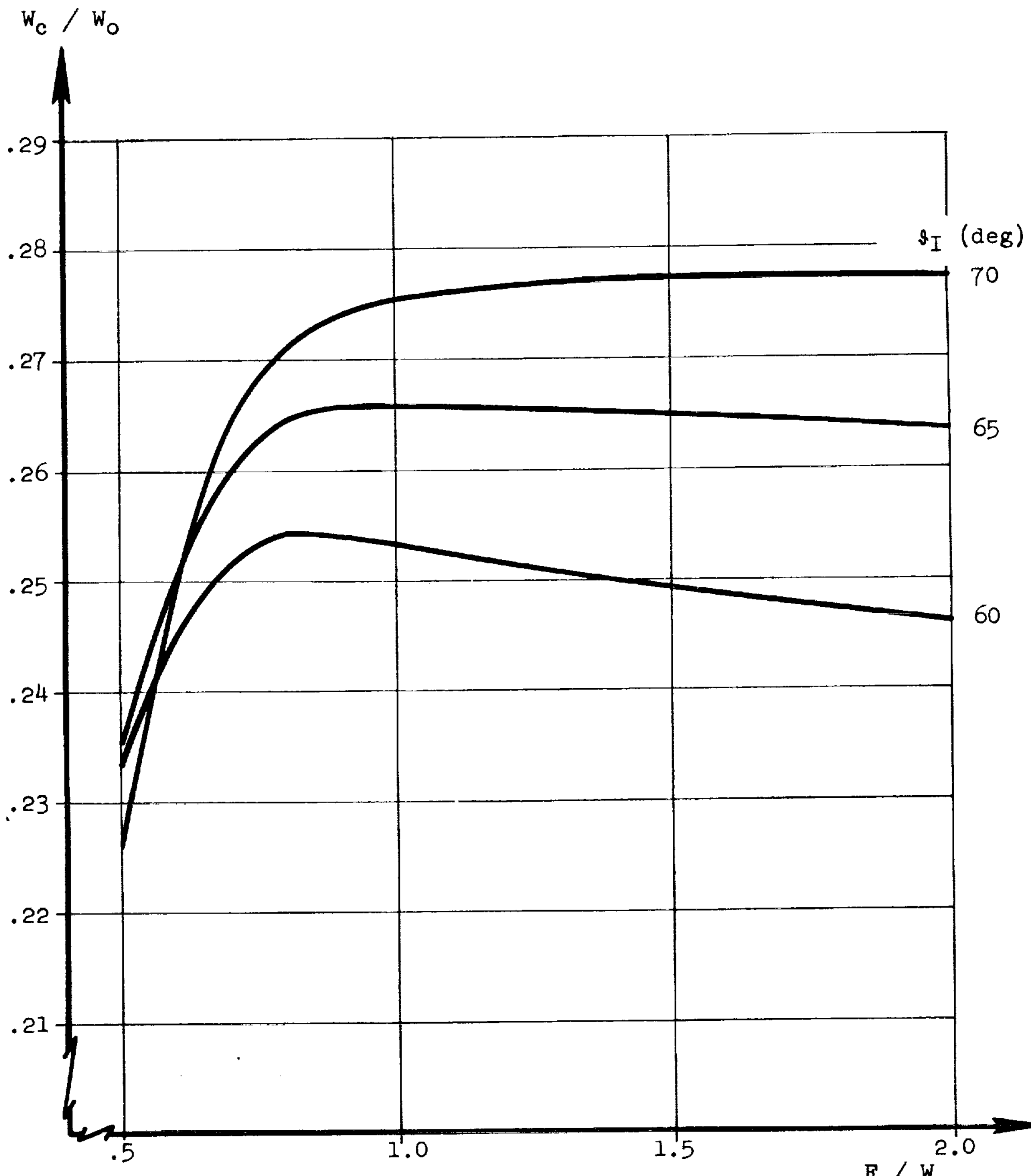

y_c = 100 km I_{sp} = 400 sec

FIGURE 29

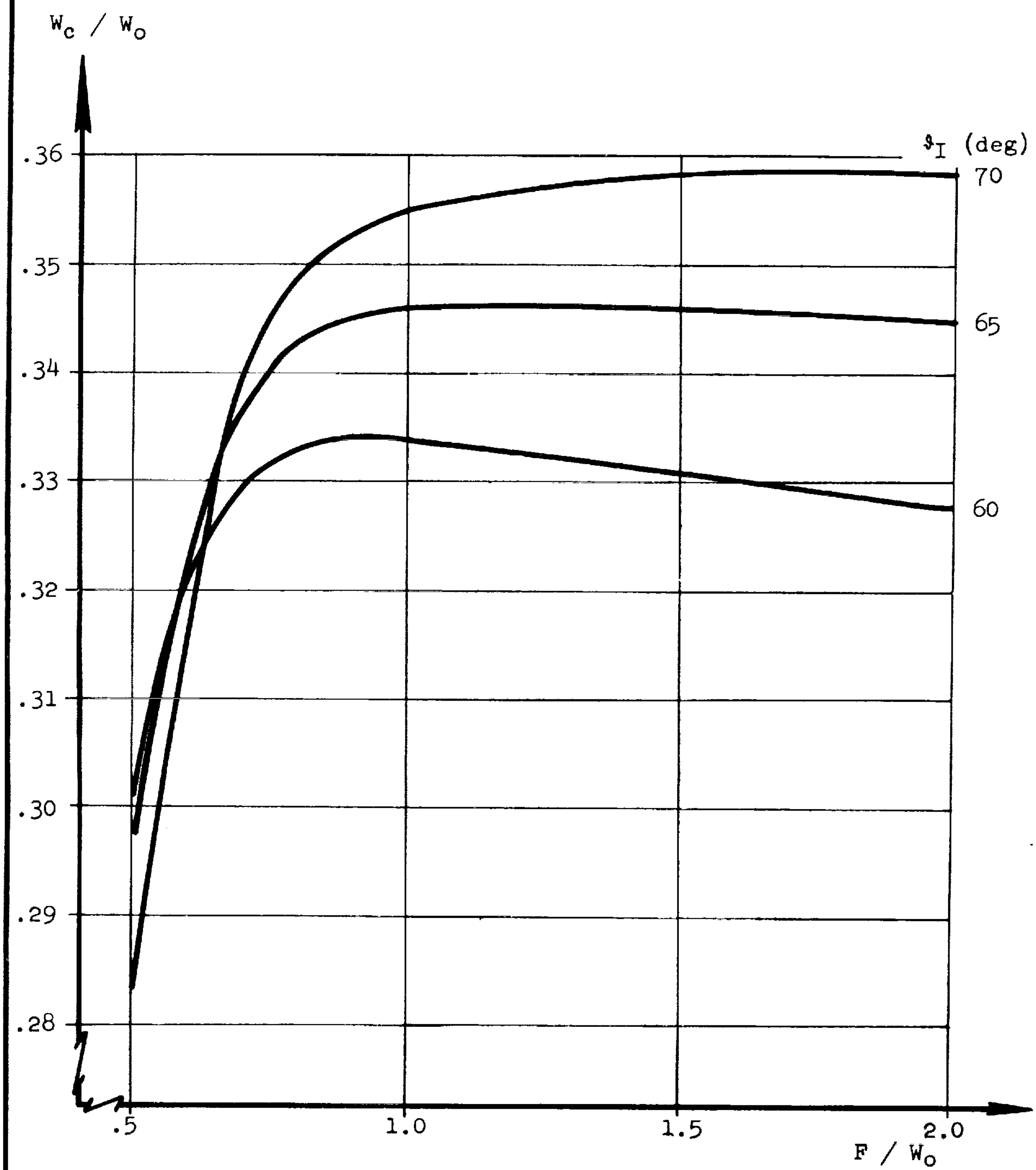

y_c = 100 km I_{sp} = 500 sec

FIGURE 30

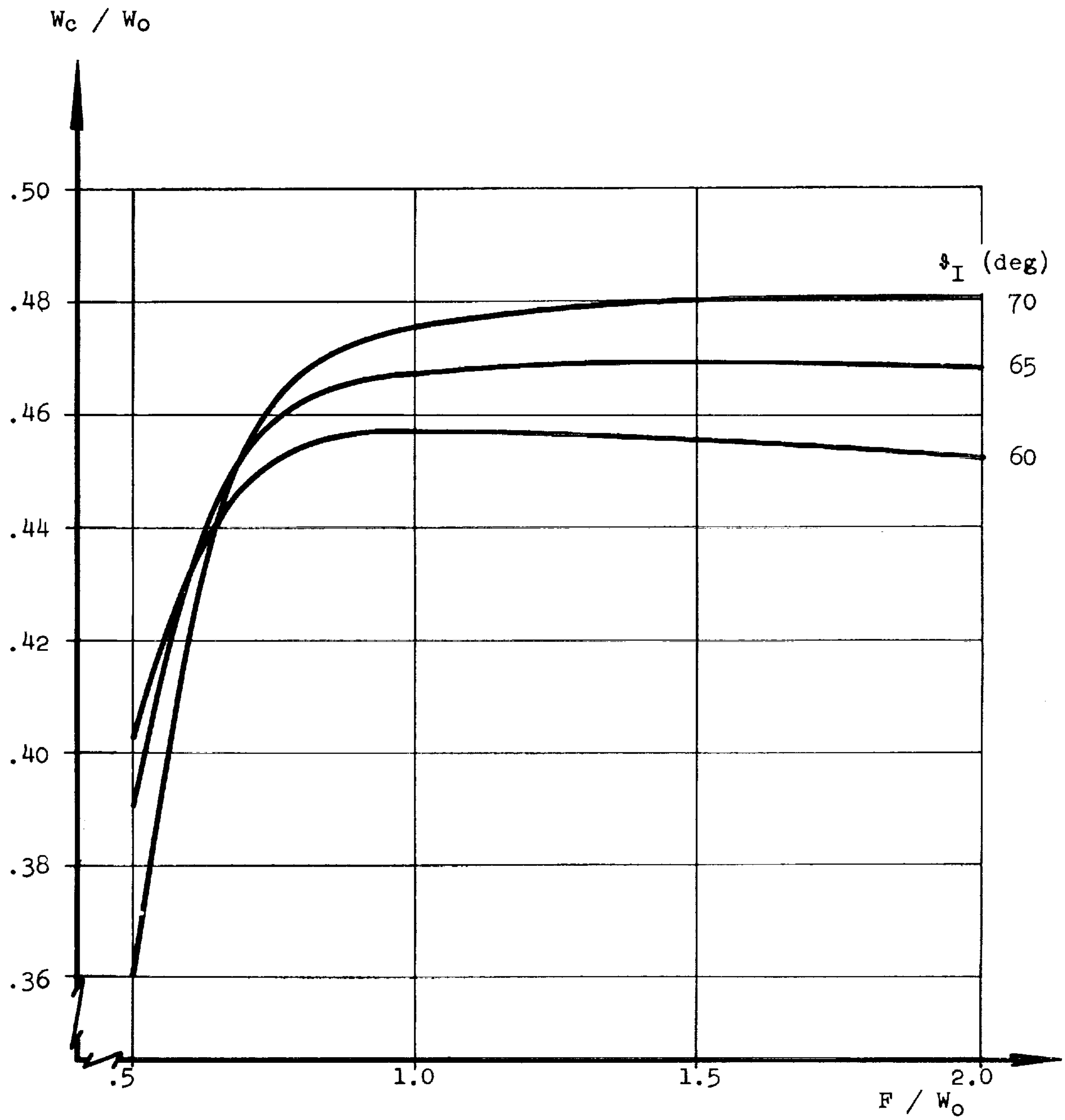

y_c = 100 km I_{sp} = 700 sec

FIGURE 31

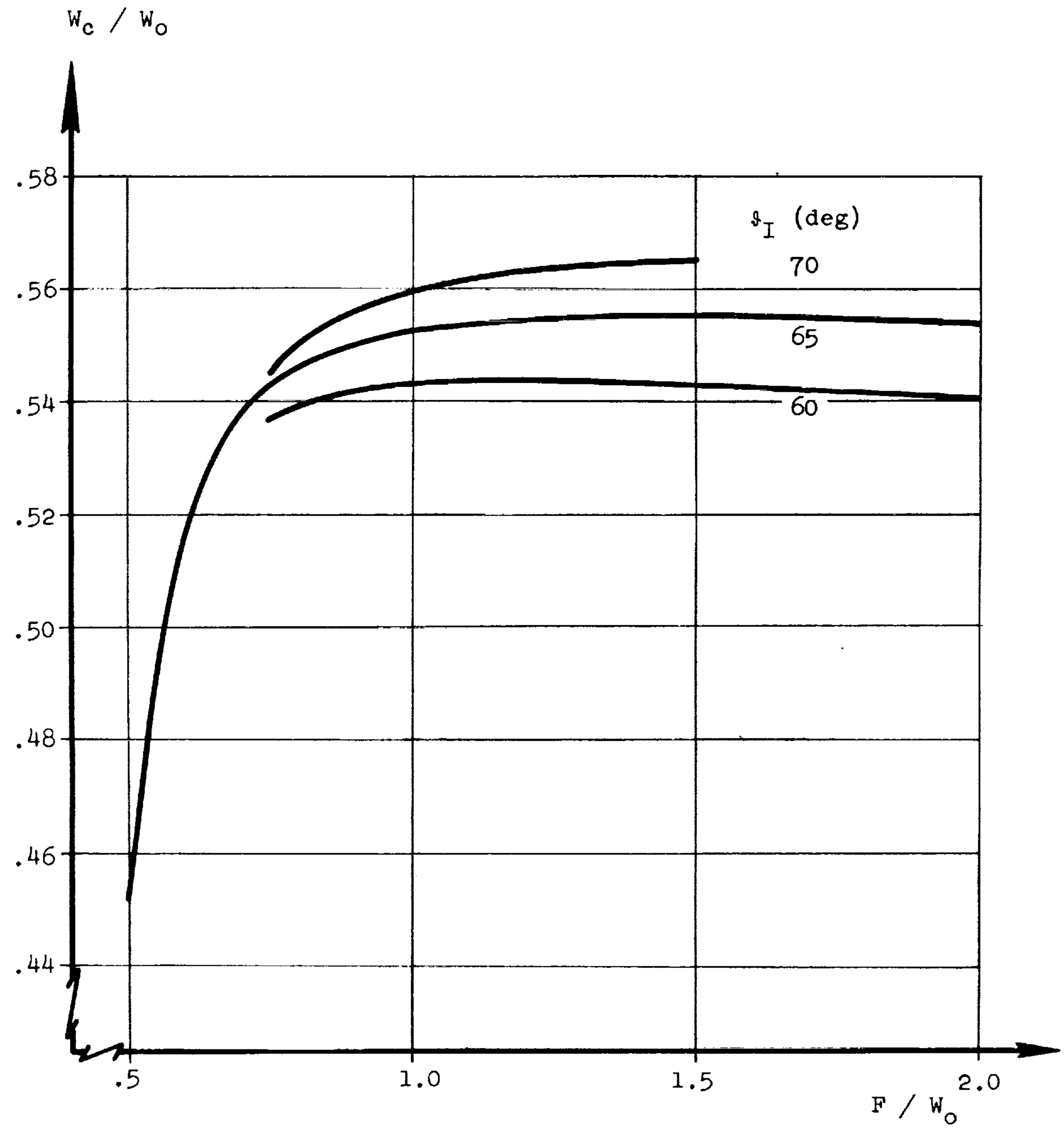

y_c = 100 km I_{sp} = 900 sec

FIGURE 32

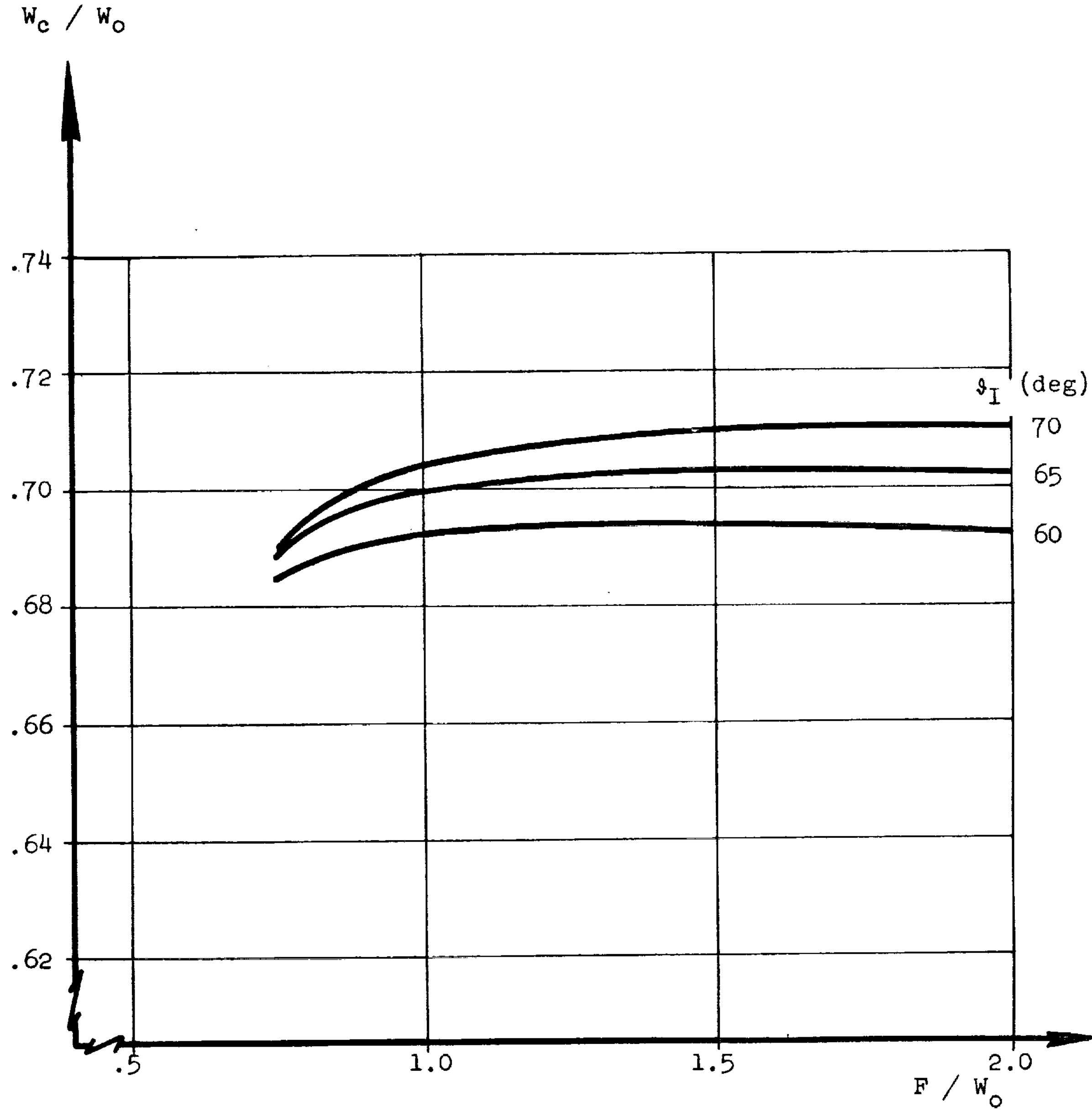

y_c = 100 km I_{sp} = 1,500 sec

FIGURE 33

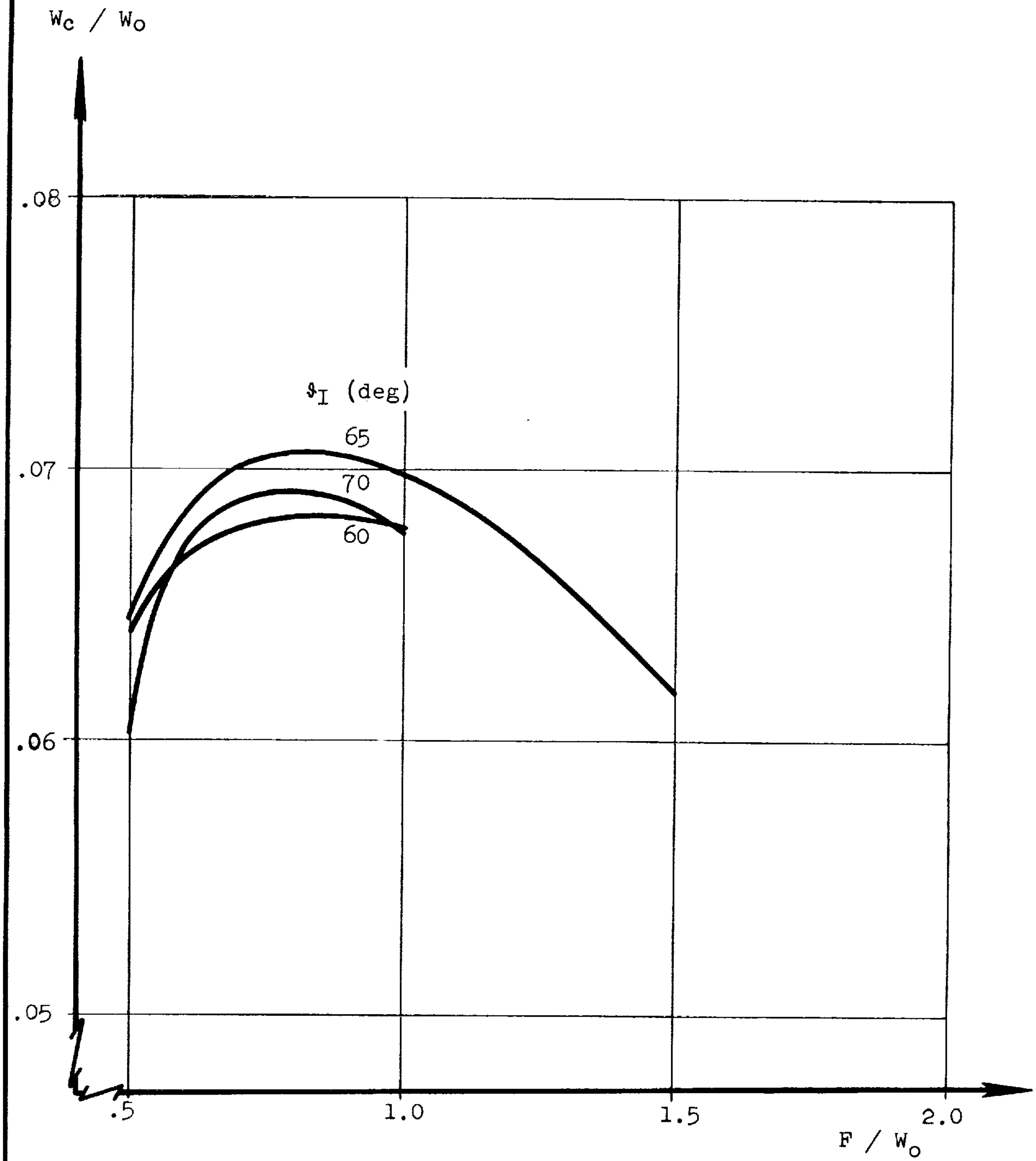

y_c = 200 km I_{sp} = 200 sec

FIGURE 34

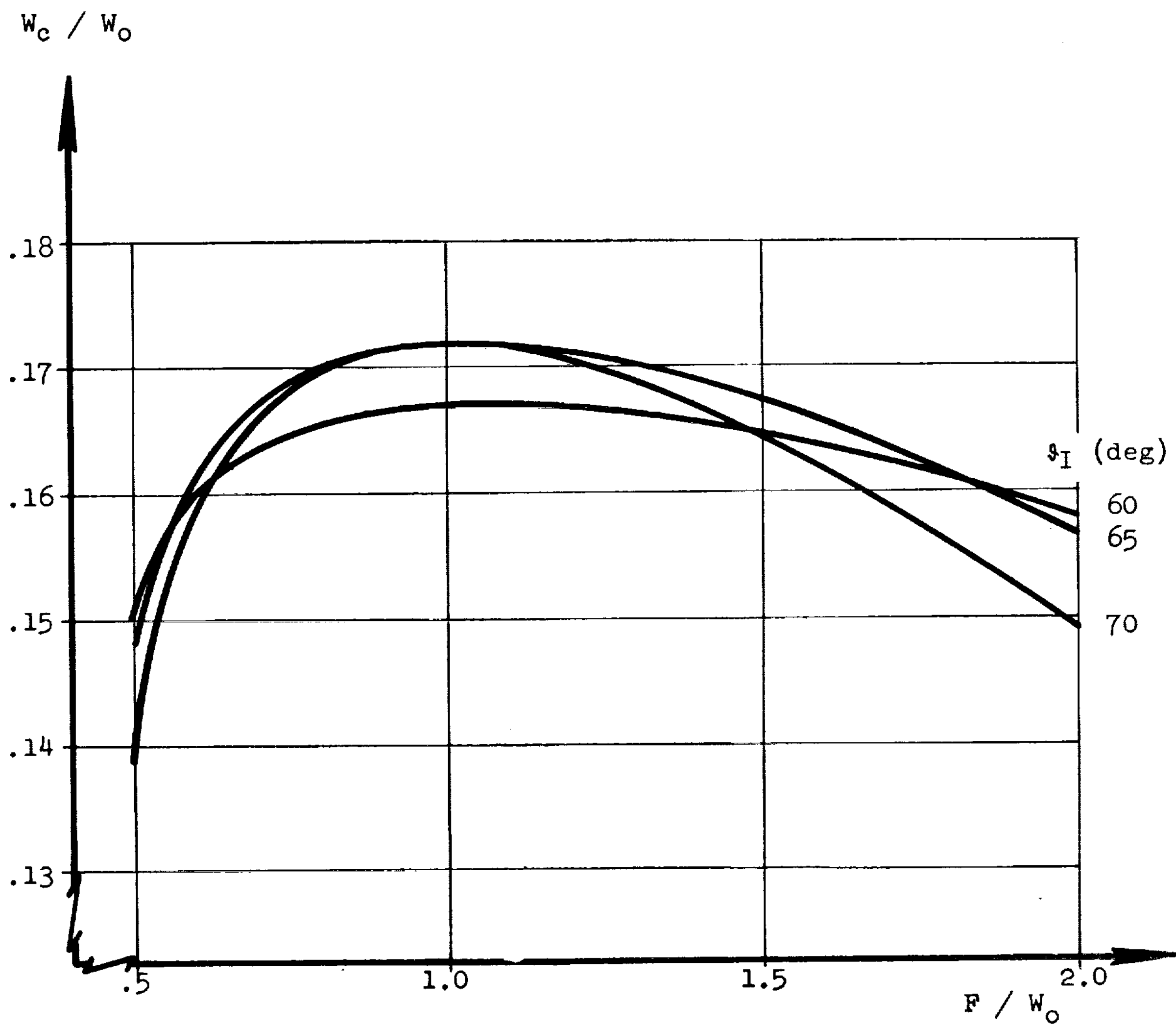

y_c = 200 km I_{sp} = 300 sec

FIGURE 35

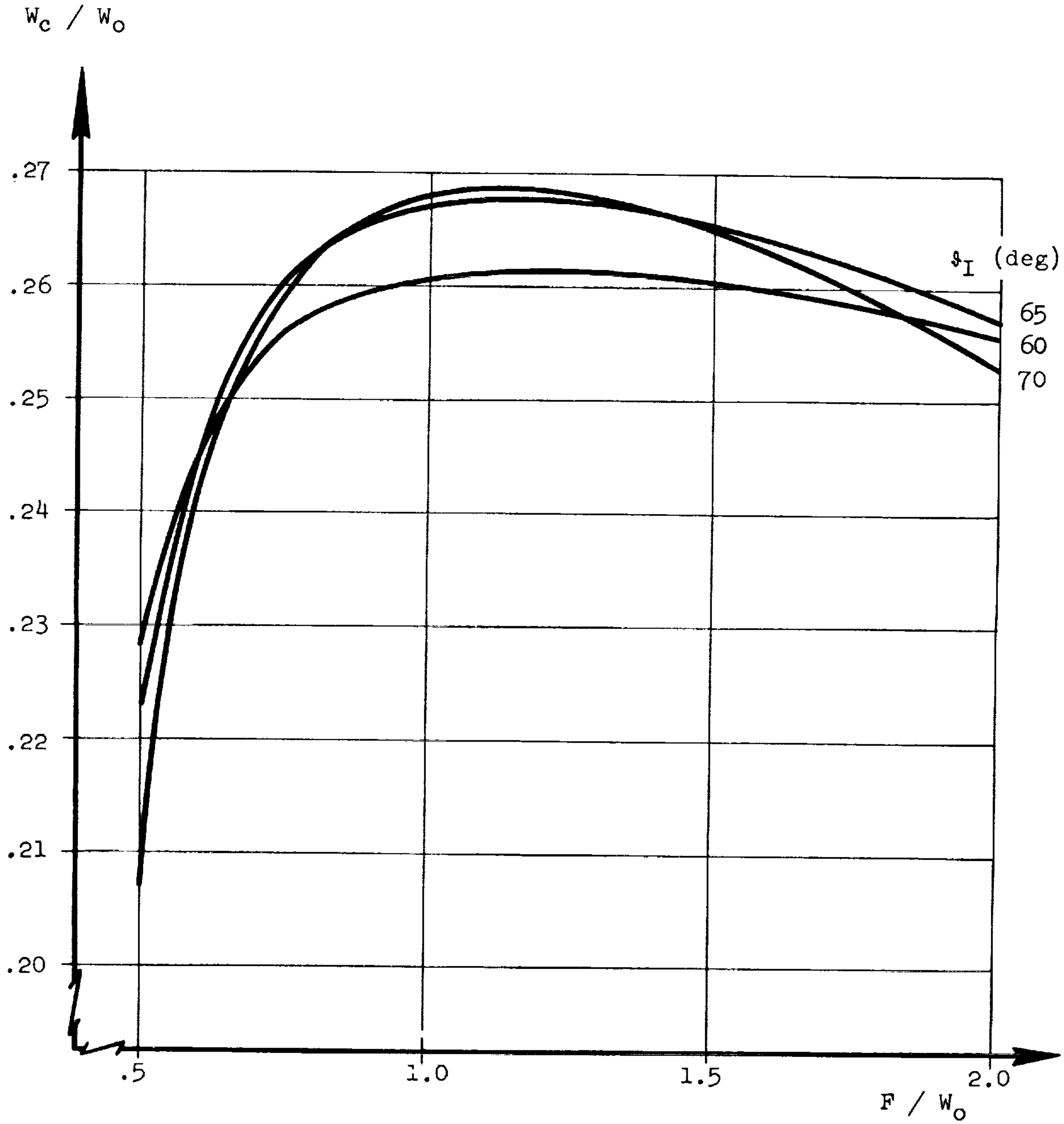

y_c = 200 km I_{sp} = 400 sec

FIGURE 36

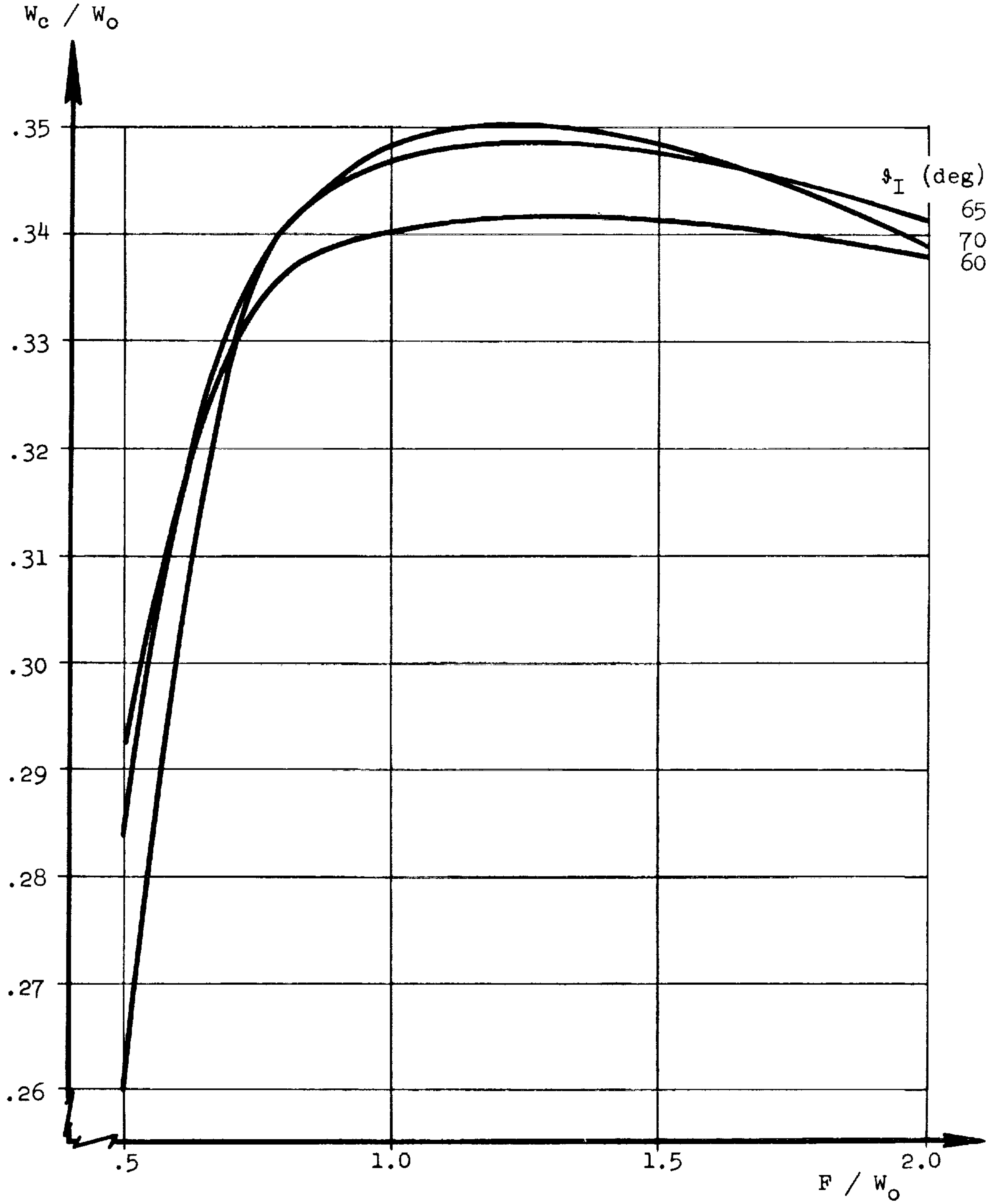

y_c = 200 km I_{sp} = 500 sec

FIGURE 37

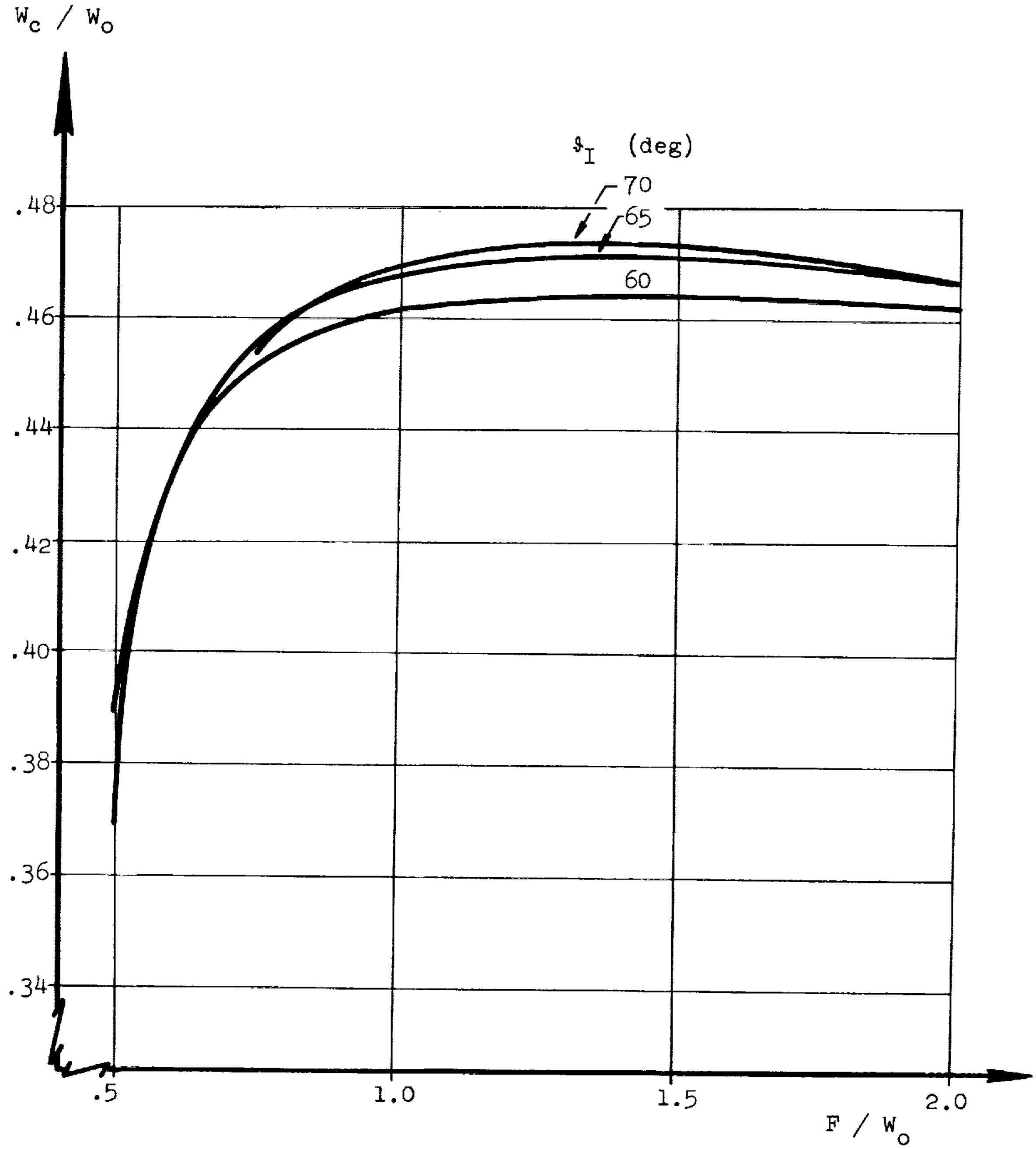

y_c = 200 km I_{sp} = 700 sec

FIGURE 38

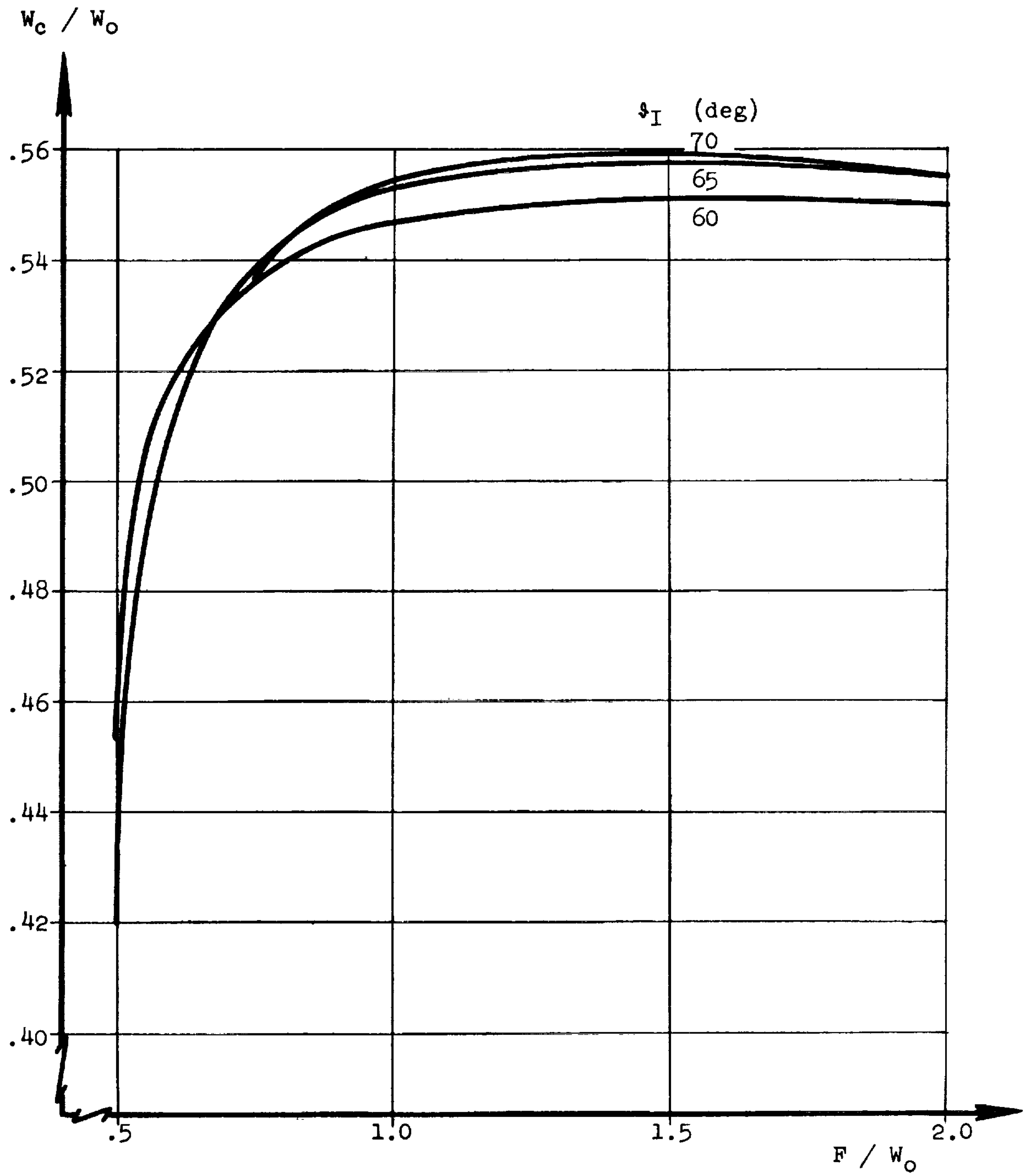

y_c = 200 km I_{sp} = 900 sec

FIGURE 39

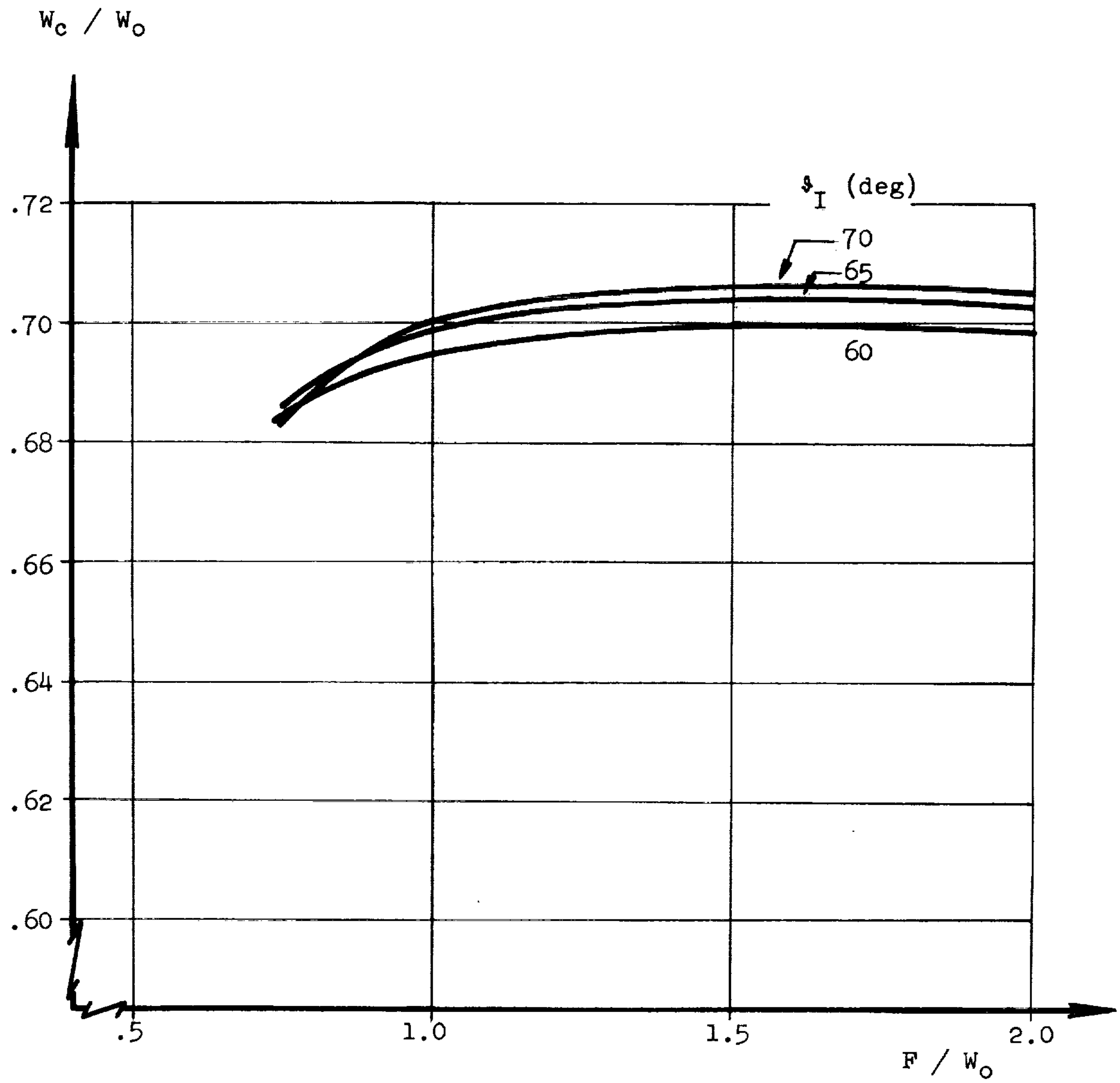

y_c = 200 km I_{sp} = 1,500 sec

FIGURE 40

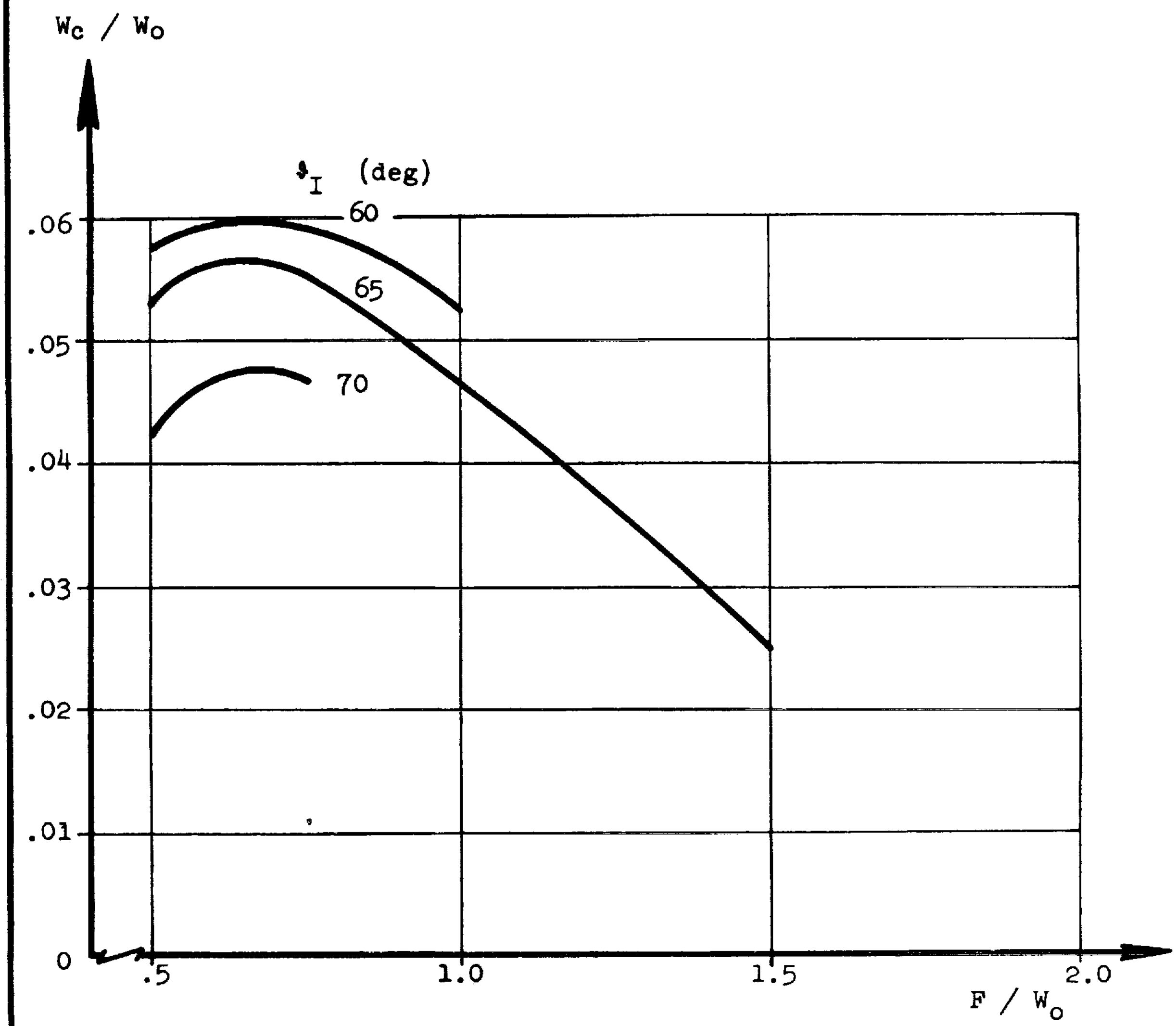

y_c = 300 km I_{sp} = 200 sec

FIGURE 41

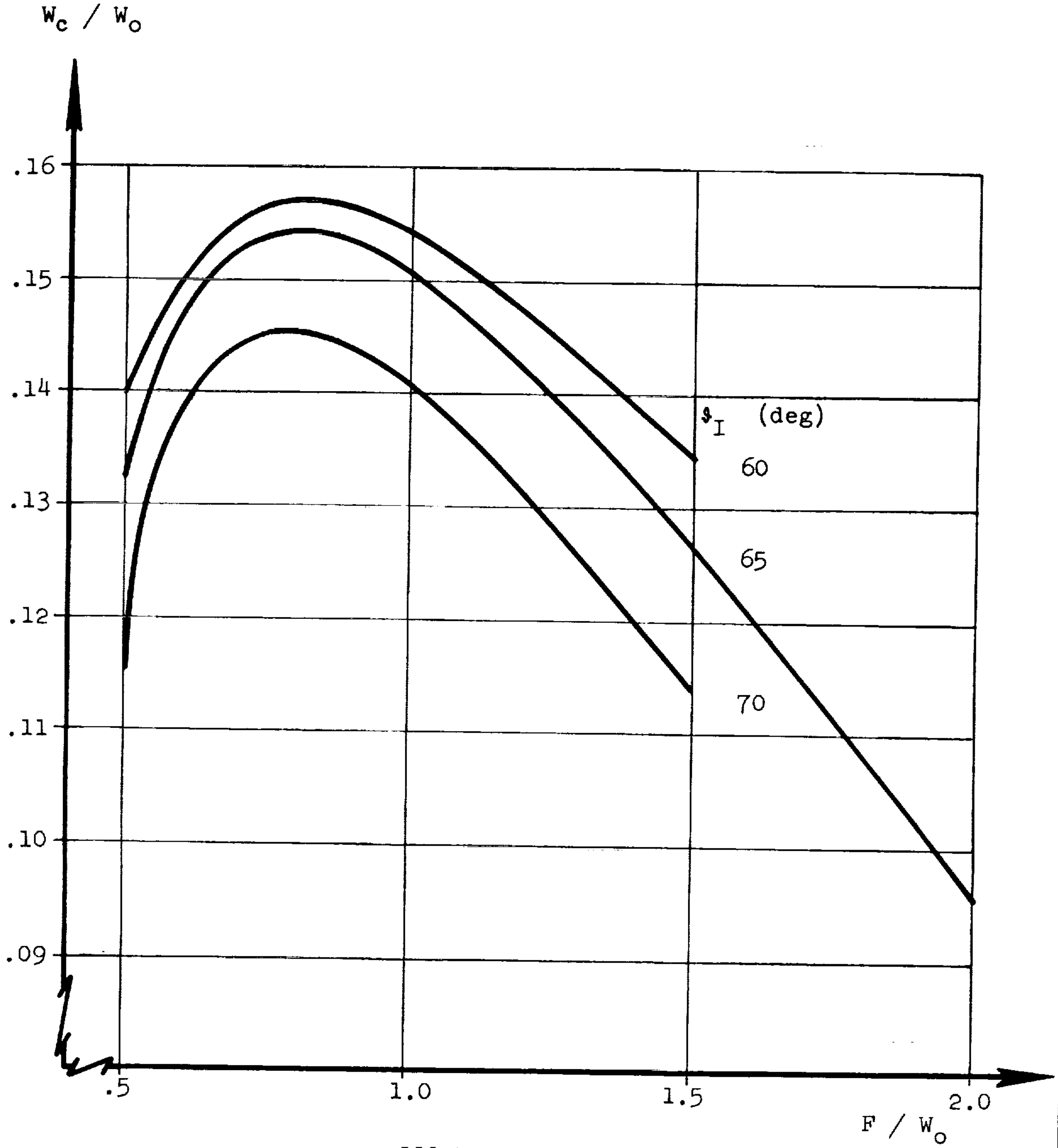

y_c = 300 km I_{sp} = 300 sec

FIGURE 42

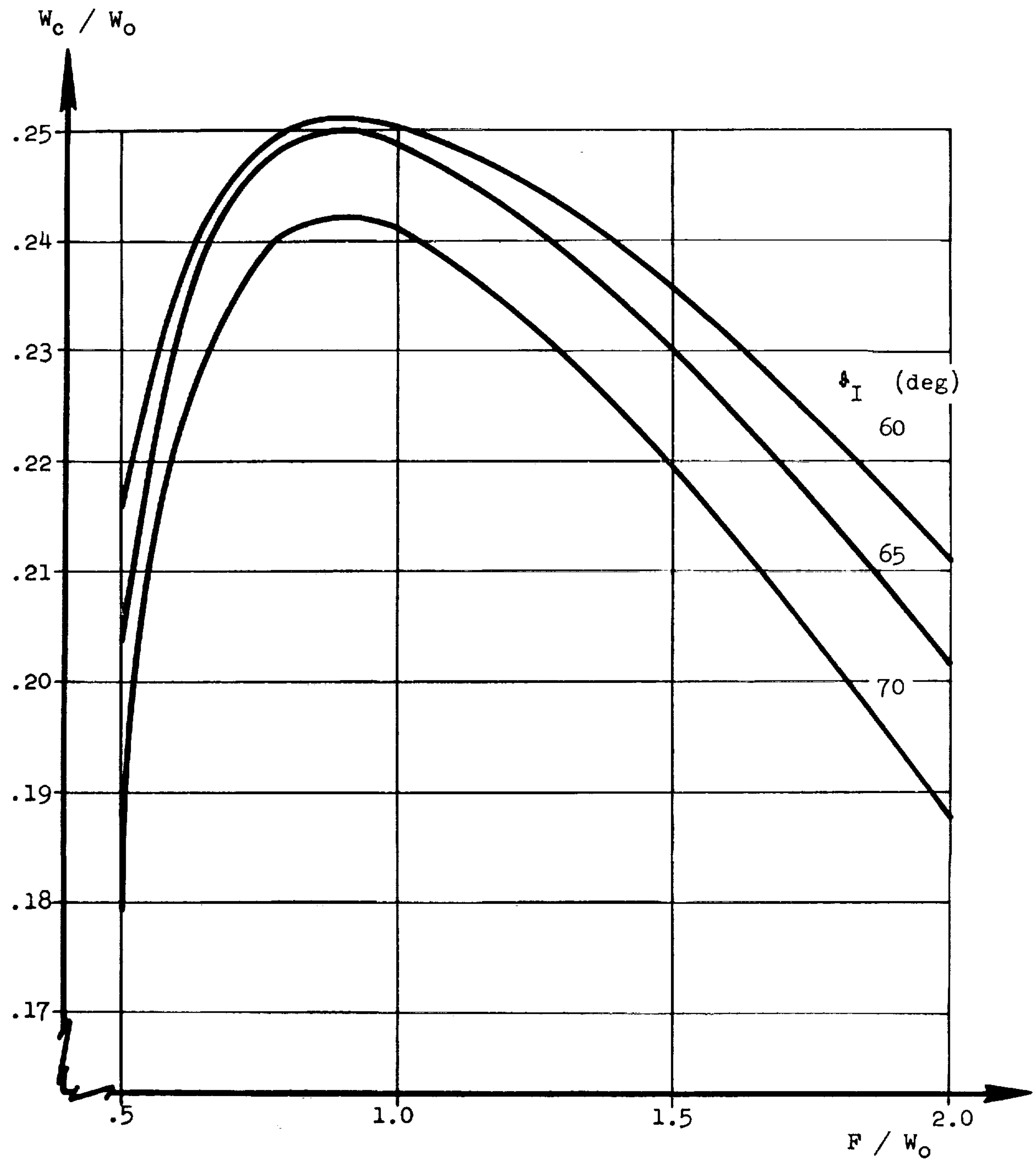

y_c = 300 km I_{sp} = 400 sec

FIGURE 43

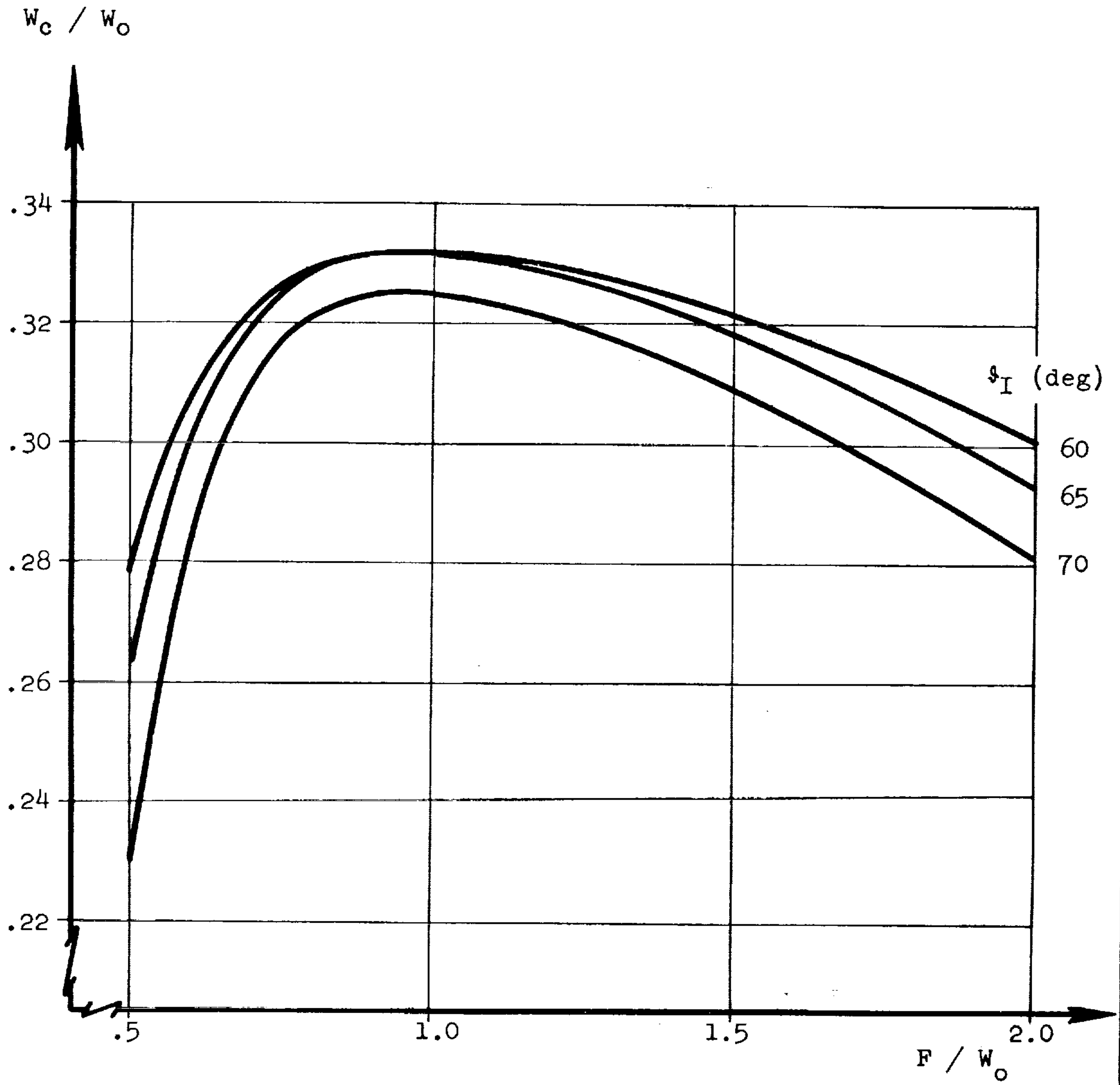

y_c = 300 km I_{sp} = 500 sec

FIGURE 44

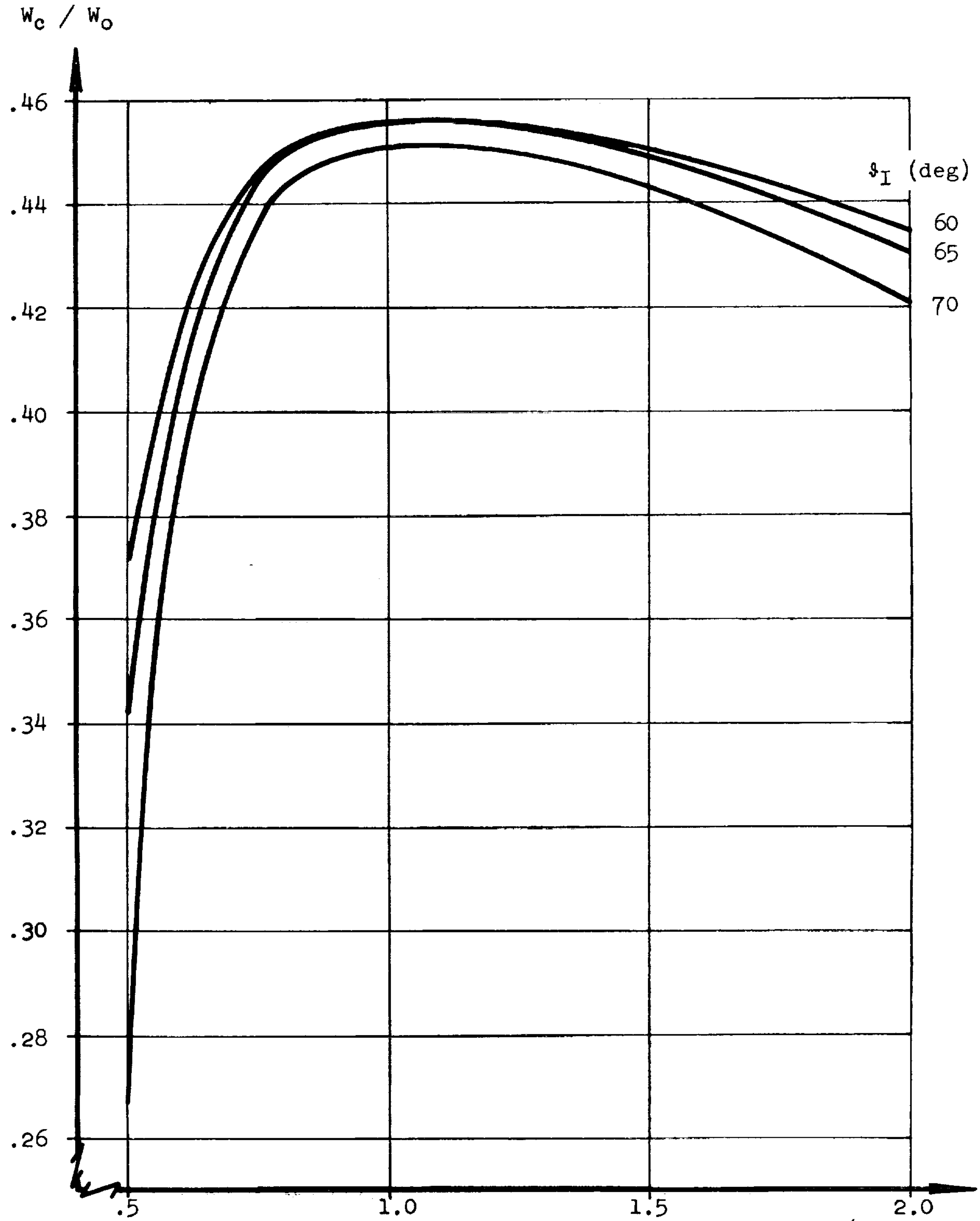

y_c = 300 km I_{sp} = 700 sec

FIGURE 45

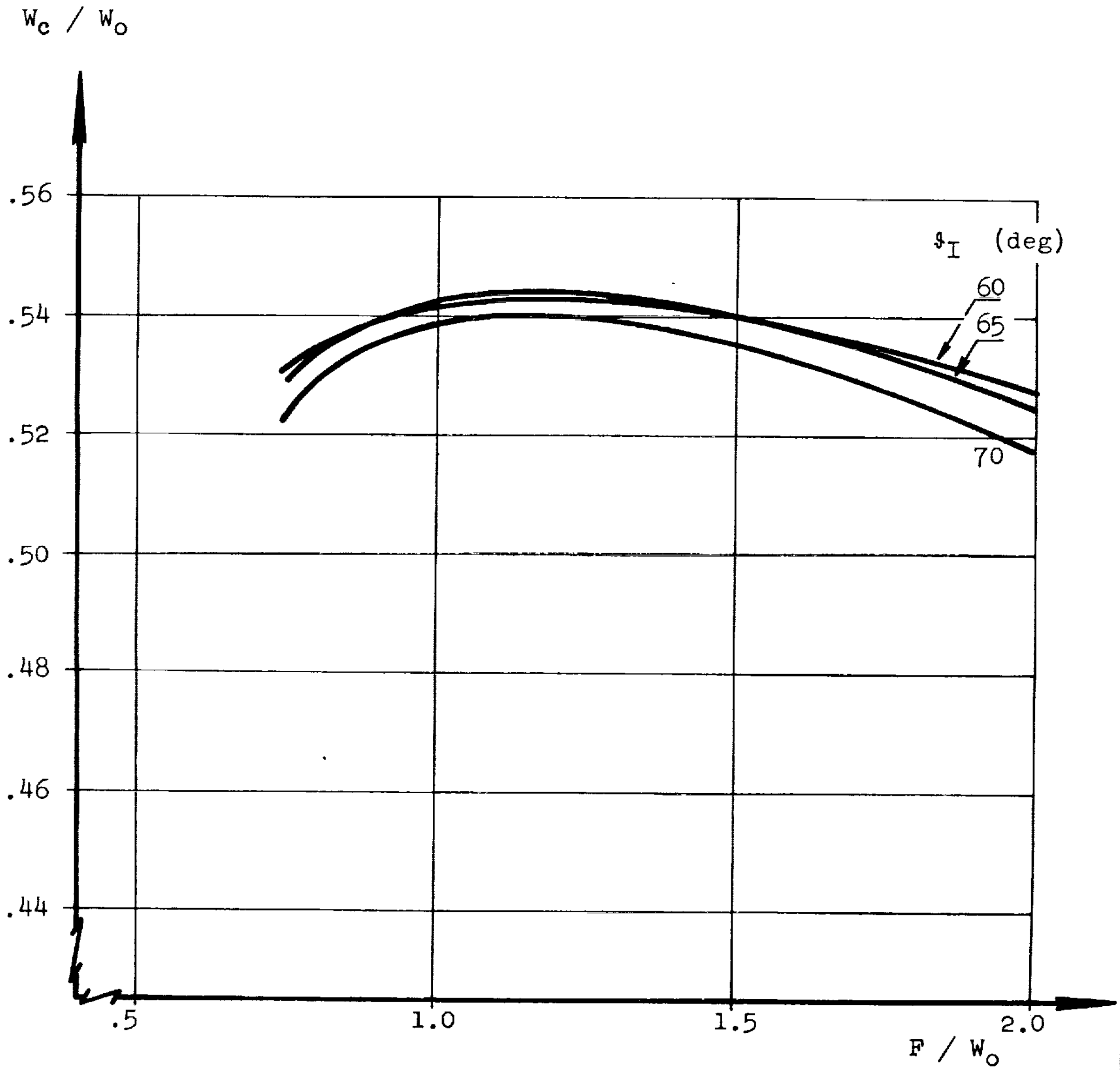

y_c = 300 km I_{sp} = 900 sec

FIGURE 46

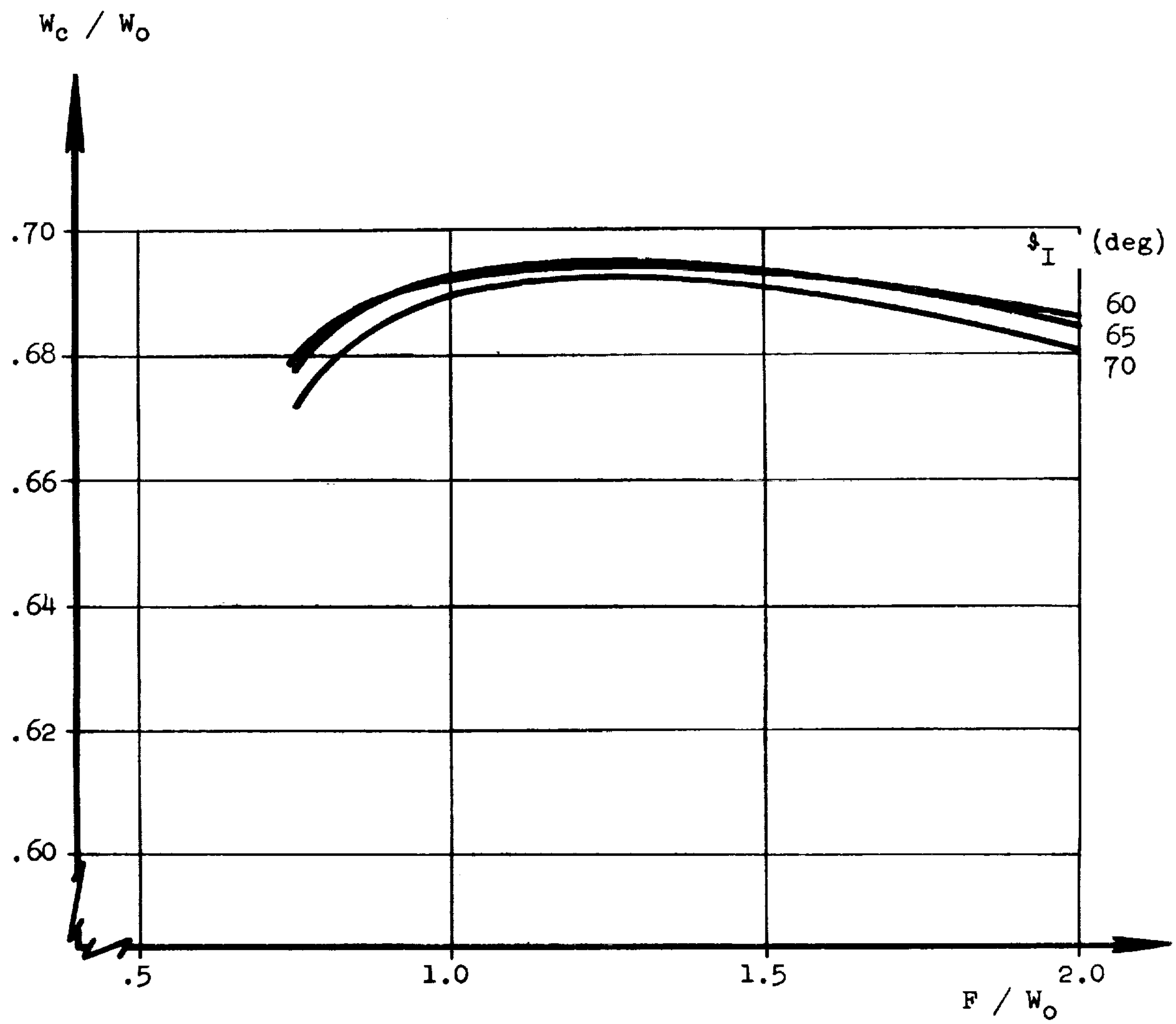

y_c = 300 km I_{sp} = 1,500 sec

FIGURE 47

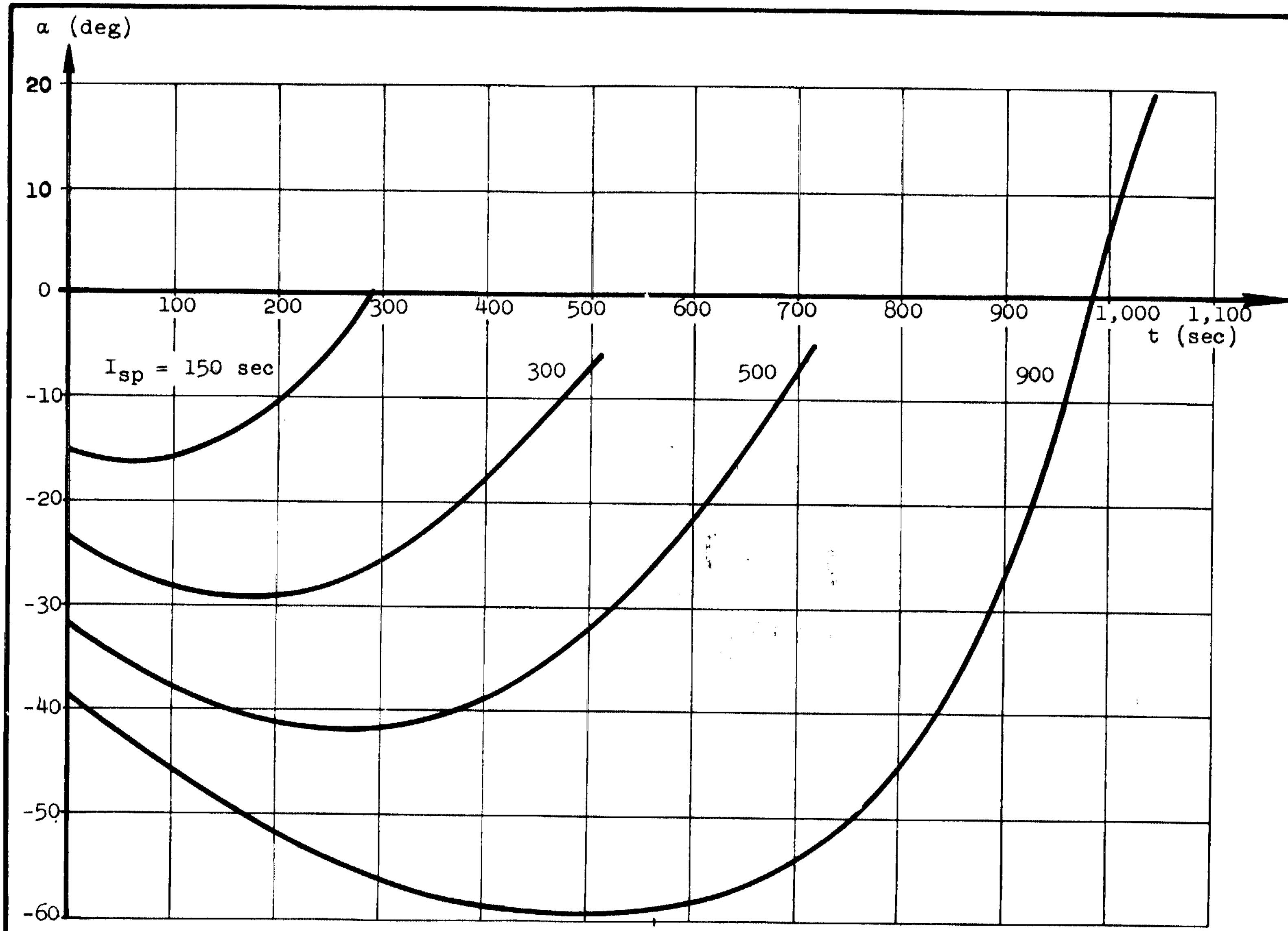

$F/W_o = 0.5$ $R_c = 200$ KM $\vartheta_I = 65$ DEG

FIGURE 48

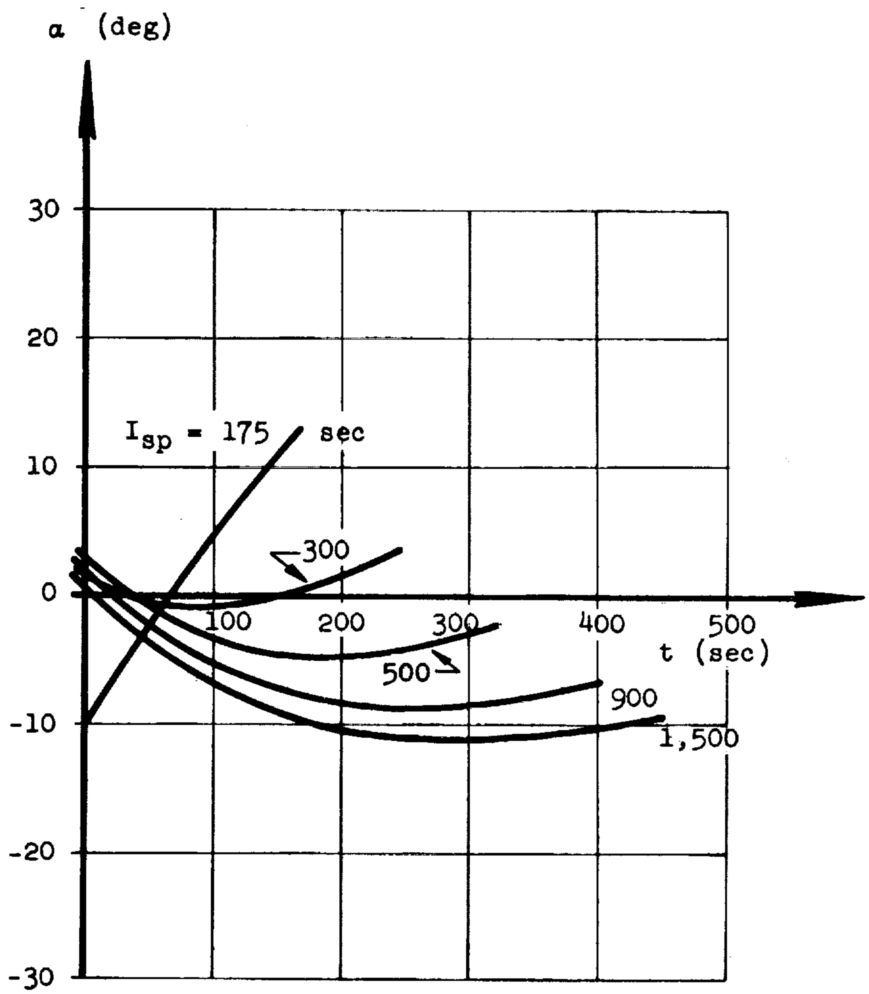

$F/W_o = 1.0$ $R_c = 200$ KM $\phi_I = 65$ DEG

FIGURE 49

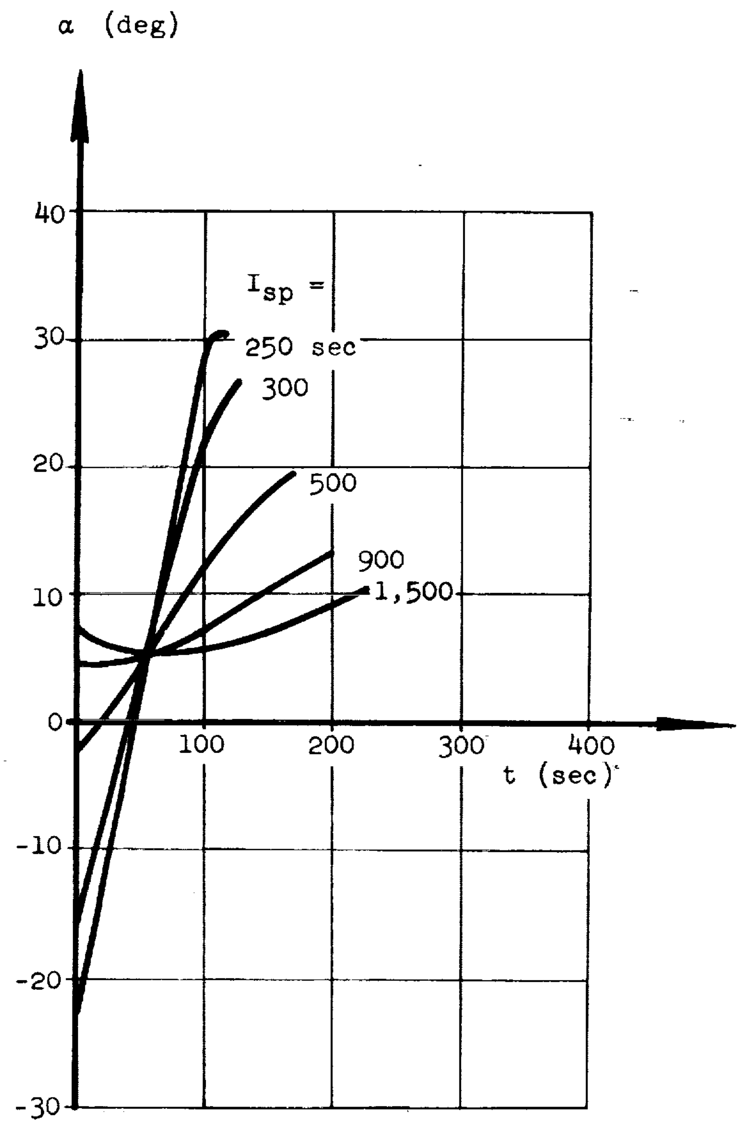

$F/W_o = 2.0$ $R_c = 200$ KM $\vartheta_I = 65$ DEG

FIGURE 50

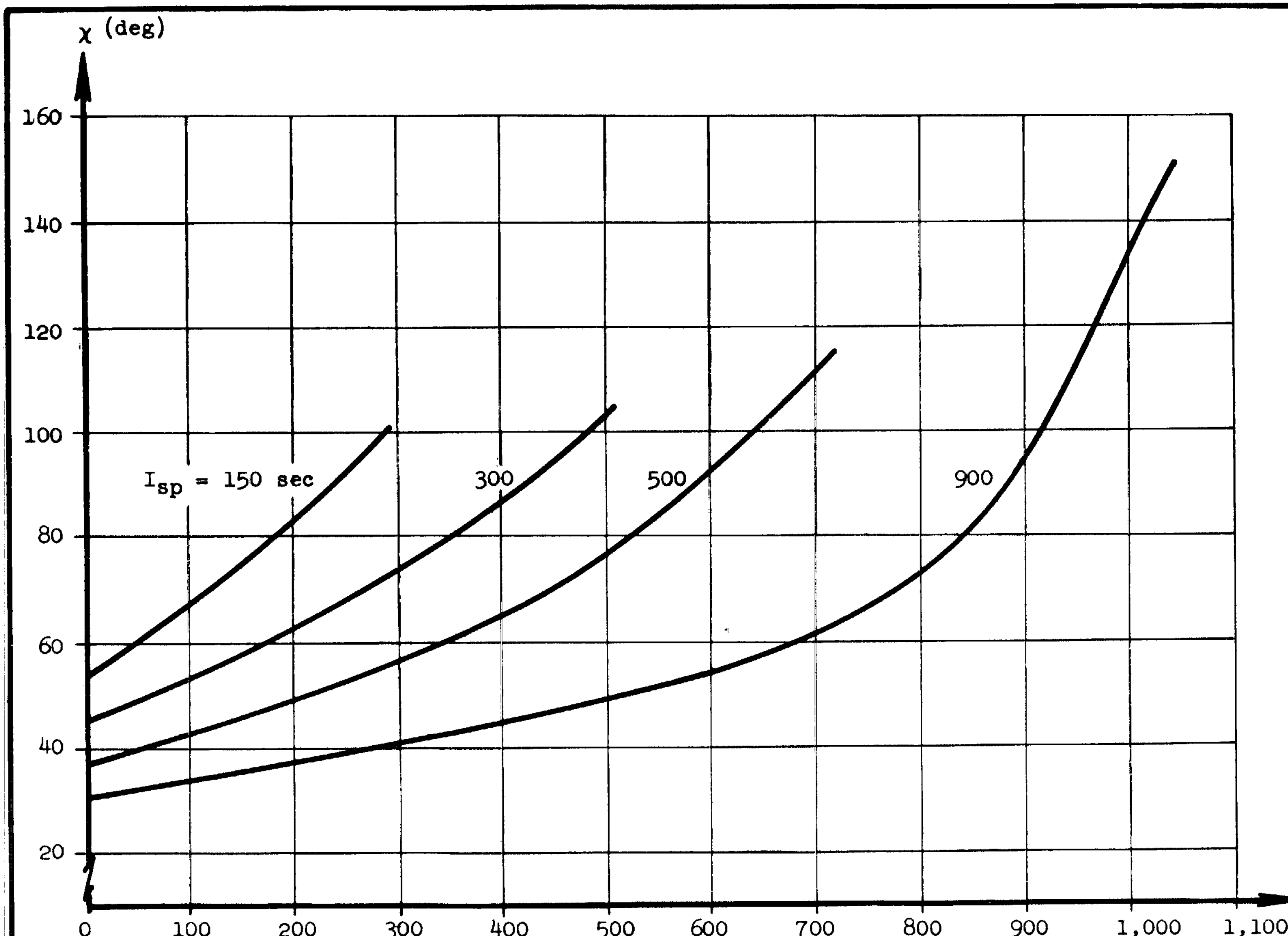

R_c = 200 km F/W_o = 1.0

FIGURE 51

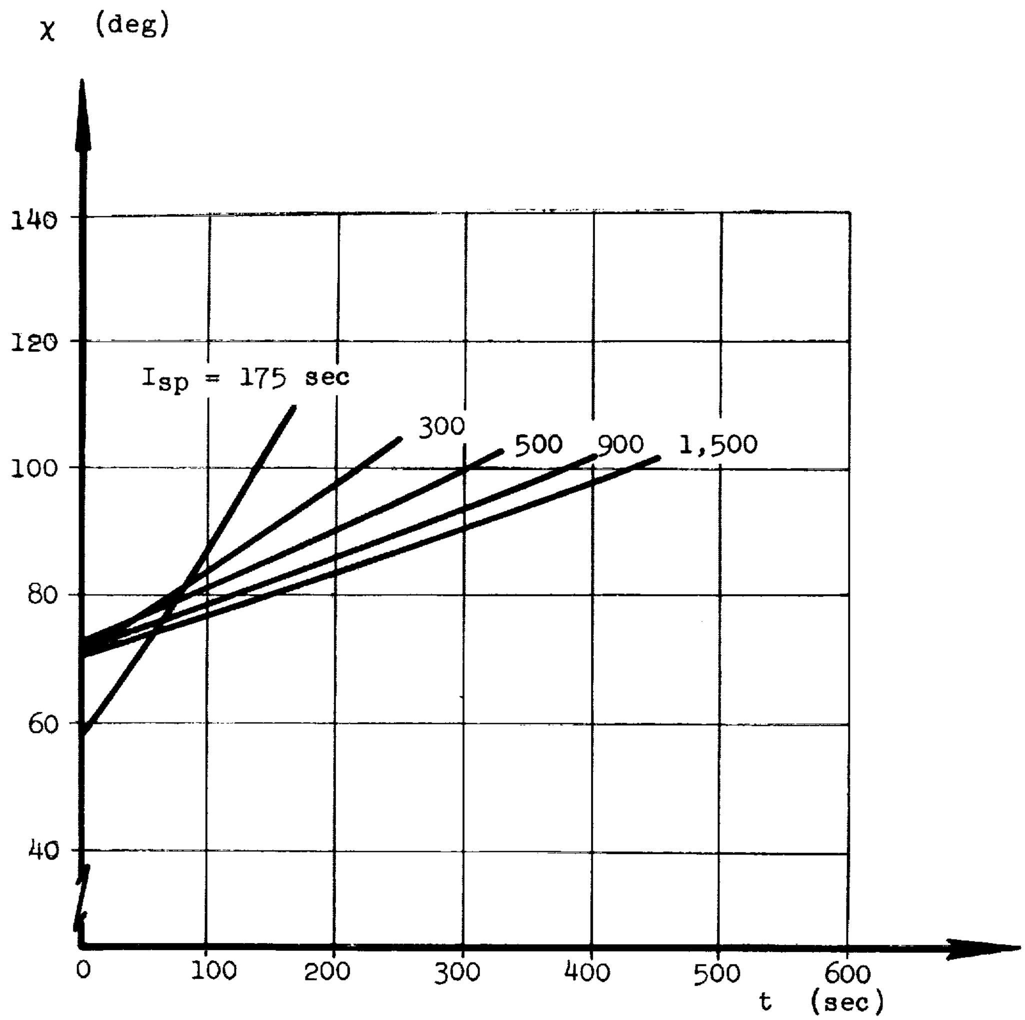

R_c = 200 km

F/W_o = 1.0

FIGURE 52

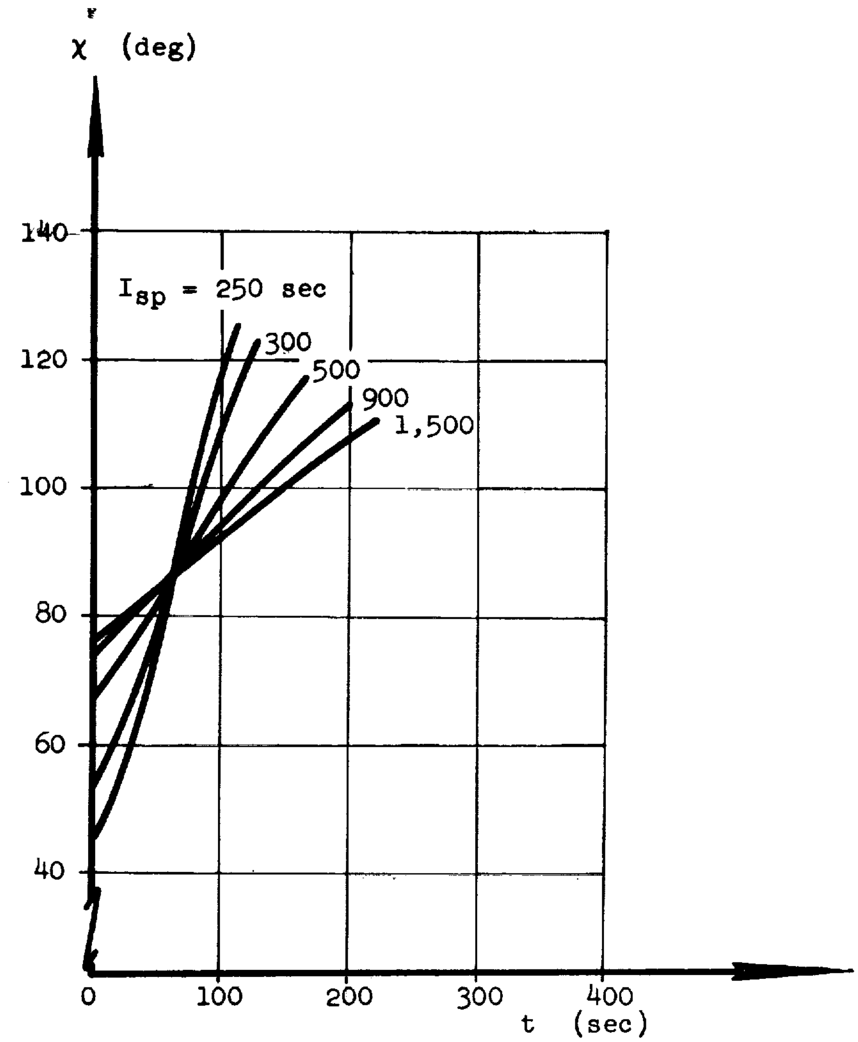

R_c = 200 km
F/W_o = 2.0

FIGURE 53

APPROVAL

A SURVEY OF THE INFLUENCE OF VARIATIONS IN STAGE CHARACTERISTICS ON OPTIMIZED TRAJECTORY SHAPING

PART I: TWO STAGE VEHICLE INJECTION INTO CIRCULAR ORBITS

By M. C. Davidson, Jr.

The information in this report has been reviewed for security classification. Review of any information concerning Department of Defense or Atomic Energy Commission programs has been made by the MSFC Security Classification Officer. This report, in its entirety, has been determined to be Unclassified.

ORIGINATOR

M. C. Davidson Jr

M. C. DAVIDSON, JR.
Aerospace Engineer

APPROVAL

John B. Winch

JOHN B. WINCH, Chief
Space Projects Section 2

APPROVAL

R. F. HOELKER, Chief
Future Projects Branch

E. D. GEISSLER, Director
Aeroballistics Division

DISTRIBUTION LIST

INTERNAL

M-DIR
M-DEP-R&D
M-RP, Dr. Johnson

M-FPO, Mr. Koelle
Dr. Ruppe

M-COMP, Dr. Arenstorf
Mr. Davidson (10)

M-P&VE, Dr. Krause
Mr. Neighbors
Mr. Galzerano
Mr. Burns
Mr. Swanson

M-ASTR, Mr. Richard
Mr. Moore
Mr. Hosenthien
Mr. Blackstone
Mr. Scofield
Mr. Brooks
Mr. Woods
Mr. Digesu
Mr. Thornton
Mrs. Neighbors

M-MS-IP
M-MS-IPL (8)
M-PAT
M-HME-P
M-MS-H

M-AERO, Dr. Geissler
Mr. Horn
Mr. Hart
Mrs. Chandler
Mr. Callaway
Mr. Thomae
Mr. Scott
Mr. Stone
Mr. Baker
Mr. Golmon
Dr. Speer
Mr. Lindberg
Mr. Kurtz
Mr. Vaughan
Mr. Jean
Mr. Thionnet
Mr. McNair
Mr. Teague
Mr. McQueen
Mr. deFries
Mr. Bombara
Dr. Hoelker
Mr. Miner
Mr. Schmieder
Mr. Silber
Mr. Dearman
Mr. Braud
Mr. Lisle
Mr. Schwaniger
Mr. Tucker
Mr. Winch (10)
Mr. Cremin
Mr. McDaniel
Mr. Goldsby

Scientific and Technical Information
Facility (2)
ATTN: NASA Representative (S-AK/RKT)
P. O. Box 5700
Bethesda, Md.